BIOCHEMICAL PHARMACOLOGY 75 (2008) 1129–1160

available at www.sciencedirect.com

ScienceDirect

journal homepage: www.elsevier.com/locate/biochempharm

Gene expression profiling elucidates a specific role for RARγ in the retinoic acid-induced differentiation of F9 teratocarcinoma stem cells

Dan Su [a,b], *Lorraine J. Gudas* [a,*]

[a] *Department of Pharmacology, Weill Cornell Medical College United States*
[b] *Pharmacology Program of Weill Graduate School of Biomedical Sciences of Cornell University, New York, NY 10021 United States*

ARTICLE INFO

Article history:
Received 29 August 2007
Accepted 15 November 2007

Keywords:
Retinoic acid receptor
Gene expression profiles
Differentiation
Retinol
sfrp5
Tie1

ABSTRACT

The biological effects of all-*trans*-retinoic acid (RA), a major active metabolite of retinol, are mainly mediated through its interactions with retinoic acid receptor (RARs α, β, γ) and retinoid X receptor (RXRs α, β, γ) heterodimers. RAR/RXR heterodimers activate transcription by binding to RA-response elements (RAREs or RXREs) in the promoters of primary target genes. Murine F9 teratocarcinoma stem cells have been widely used as a model for cellular differentiation and RA signaling during embryonic development. We identified and characterized genes that are differentially expressed in F9 wild type (Wt) and F9 RARγ$^{-/-}$ cells, with and without RA treatment, through the use of oligonucleotide-based microarrays. Our data indicate that RARγ, in the absence of exogenous RA, modulates gene expression. Genes such as Sfrp2, Tie1, Fbp2, Emp1, and Emp3 exhibited higher transcript levels in RA-treated Wt, RARα$^{-/-}$ and RARβ$_2^{-/-}$ lines than in RA-treated RARγ$^{-/-}$ cells, and represent *specific* RARγ targets. Other genes, such as Runx1, were expressed at lower levels in both F9 RARβ$_2^{-/-}$ and RARγ$^{-/-}$ cell lines than in F9 Wt and RARα$^{-/-}$. Genes specifically induced by RA at 6 h with the protein synthesis inhibitor cycloheximide in F9 Wt, but not in RARγ$^{-/-}$ cells, included Hoxa3, Hoxa5, Gas1, Cyp26a1, Sfrp2, Fbp2, and Emp1. These genes represent specific *primary* RARγ targets in F9 cells. Several genes in the Wnt signaling pathway were regulated by RARγ. Delineation of the receptor-specific actions of RA with respect to cell proliferation and differentiation should result in more effective therapies with this drug.

1. Introduction

Retinoids are a group of natural or synthetic derivatives of vitamin A (retinol) which include all-*trans*-, 9-*cis*- and 13-*cis*-retinoic acids (RA, 9cRA and 13cRA, respectively). Synthesis of RA, the main biologically active metabolite of vitamin A, involves the irreversible oxidation of retinol in target cells [1,2]. Retinoids are involved in multiple physiological processes including reproduction, embryonic development, epithelial differentiation, immune function, and vision [3]. In addition, retinoids modulate both normal and neoplastic cell growth through the regulation of cell differentiation and/or induction of apoptosis [4,5].

The biological effects of RA are thought to be primarily mediated through interactions with retinoic acid receptors (RARs) or retinoic X receptors (RXRs), which function as transcription factors that activate transcription by binding to RA-response elements (RAREs or RXREs) in the promoter

* *Corresponding author* at: Department of Pharmacology, Weill Cornell Medical College, 1300 York Avenue, Room E-409, New York, NY 10065, United States. Tel.: +1 212 746 6250; fax: +1 212 746 8858.
E-mail address: ljgudas@med.cornell.edu (L.J. Gudas).
0006-2952/$ – see front matter
doi:10.1016/j.bcp.2007.11.006

regions of target genes [6]. Both RARs and RXRs exhibit three isotypes, α, β, and γ, which are encoded by different genes. Each isotype has several isoforms produced from differential splicing and alternative use of promoters [7,8]. All-*trans*-retinoic acid (RA) binds and activates RARs, while 9-*cis*-retinoic acid binds and activates both RARs and RXRs. The multiple RARs and RXRs are conserved in vertebrate evolution and display distinct spatial–temporal expression patterns in developing embryos and adult tissues [9,10]. Although gene disruption studies in mice have revealed some functional redundancy among the different RAR isotypes [11,12], each RAR isotype performs unique functions in development and differentiation which cannot be replaced by the actions of the other isotypes [11,12]. RARγ plays a major role in axial rotation and vertebra specification [13], hindbrain patterning (specification of rhombomere 5/6 territory) [14], epidermal hyperplasia [15,16], formation of otocysts, pharyngeal arches and the forelimb bud, closure of the primitive gut, cardiac looping morphogenesis [17], alveoli regeneration [18], hematopoietic stem cell self-renewal [19], and inflammatory cytokine production [20]. In addition, activation of RARγ is essential for induction of apoptosis in melanoma cells [21], neuroblastoma cells [22], neoplastic epidermal cells [23], and human pancreatic cancer cells [24]. In melanoma cells, RARγ-selective compounds were able to induce apoptosis and differentiation [25]. However, the molecular mechanisms by which RARγ induces apoptosis and growth inhibition in these tumor cells are not well defined.

To delineate the specific roles of RARγ in retinoid signaling, the identification of specific RARγ target genes is crucial. The F9 teratocarcinoma stem cell line is a good model for investigating the mechanism by which RA induces cell differentiation and controls cell proliferation [26]. Upon exposure to RA, F9 Wt cells differentiate into primitive endoderm-like cells, with differentiation markers that resemble those in early embryos [27–29]. In our laboratory F9 RARα$^{-/-}$, RARβ$_2$$^{-/-}$ and RARγ$^{-/-}$ cell lines have been generated by homologous recombination [30–33]. The F9 RARγ null cells are unable to differentiate fully [30,34]. Based on our previous findings and those of other researchers that the expression of some RA-inducible genes, such as Hoxa1, Hoxa3, laminin B1, Cdx1, collagen IV (α1), GATA-4, BMP-2, and Cyp26a1, is reduced in the RARγ$^{-/-}$ F9 cells [11,30,34,35], we wanted to explore the effect of the loss of RARγ on gene transcription on a genome-wide scale. Thus, we compared the global gene expression profiles of F9 Wt *versus* RARγ$^{-/-}$ cells using Affymetrix oligonucleotide arrays (MG-U74Av2 and MG-430.2). These experiments uncovered new molecular actions of RARγ in F9 cell differentiation and provided insights into the molecular mechanisms by which RA causes cell differentiation.

2. Materials and methods

2.1. Chemicals

RA and cycloheximide were purchased from Sigma, St. Louis, MO.

2.2. Cell culture, RA, cycloheximide treatment and RNA preparation

F9 Wt, RARγ$^{-/-}$ [30], RARα$^{-/-}$ [32] and RARβ$_2$$^{-/-}$ [31] cells were grown in Dulbecco's modified Eagle's medium (DMEM) supplemented with 5% bovine calf serum, 5% fetal calf serum and 2 mM glutamine. Tissue culture flasks and plates were gelatinized with 0.3% gelatin solution for at least 5 min prior to plating. 2.0×10^6 cells were plated in 100 mm tissue culture plates for 16 h before RA or vehicle (ethanol) treatment. For cycloheximide treatment, cells were pre-treated with cycloheximide at 1 μg/ml for 20 min before RA or vehicle (ethanol) was added for a further incubation for 5.5 h. RA was dissolved in 100% ethanol, filter (0.2 μm) sterilized, and diluted in cell culture medium to a final concentration of 1×10^{-6} M. Control samples were cultured in the same volume of ethanol (vehicle) used for the RA-treated samples. The final concentration of ethanol in all experiments did not exceed 0.1 vol.%. All experiments involving RA were performed in dim light. Total cellular RNA was extracted using Trizol (Invitrogen, P/N 15596026) by following the manufacturer's protocol.

2.3. DNA microarray analyses

Microarray analysis was carried out according to the Affymetrix Genechip® expression analysis technical manual. The extracts of total RNA were cleaned up with RNeasy Mini Kit (QIAGEN) according to the manufactors's protocol. Total RNA (30 μg) from RA-treated (1 μM RA for 24 h), or RA plus cycloheximide-treated (1 μg/ml for 6 h) F9 Wt and F9 RARγ$^{-/-}$cells was reverse transcribed into cDNA. After second-strand synthesis, cDNAs were then *in vitro* transcribed into cRNAs with biotinylated ribonucleotides (Enzo Diagnostics, Farmingdale, NY). cRNA (20 μg) was fragmented by heating at 94 °C for 35 min. A cocktail containing fragmented cRNA, control oligonucleotide B2, control cRNA (Biotin B, Biotin C, Biotin D, and Cre, Hybridization Control Kit, Affymetrix, P/N 900454),), and herring sperm DNA was hybridized to microarray chip MG-U74Av2 (Affymetrix, P/N 900344), which covers 36,000 mouse transcripts and variants representing 12,488 genes, for 16 h at 45 °C. In a second study, 15 μg of total RNA from vehicle (ethanol)-treated or RA (1 μM for 24 h)-treated F9 Wt and F9 RARγ$^{-/-}$ cells was reverse transcribed into cDNA and then *in vitro* transcribed into cRNAs. Fragmented cRNAs (15 μg) were hybridized to microarray chip MG-430.2 array (Affymetrix, P/N 900496) which covers the transcribed mouse genome with over 45,000 transcripts representing 34,000 well-substantiated mouse genes. The hybridized microarray chips were washed and stained in a Fluidics station, and were scanned by the GeneArray™ Scanner in the Microarray Core Facility at Weill Cornell Medical College. The resultant images were processed with MAS (Microarray Suite) 5.0 software (Affymetrix, Santa Clara, CA). The microarray experiments were repeated two or three times with different RNA preparations, and the overall data from the three independent experiments were further analyzed using the GeneSpring v7.0 (Silicon Genetics) software package. These data have been deposited in the GEO database (www.ncbi.nlm.nih.gov/geo, accession # GSE8431).

A three-step normalization algorithm was used in the GeneSpring software analysis. In the first step, data transformation of all data less than 0.01 was reset to 0.01. In the second normalization step, each chip was normalized to the 50th percentile intensity of total intensity. In the third step, per gene normalization was done by dividing the median intensity of that gene in several control samples. A Welch's *t*-test with a cutoff of a *P*-value ≤ 0.05 in a cross-gene error model was applied to select those statistically significant genes between two groups.

2.4. Semi-quantitative and quantitative real-time RT-PCR

Total RNA (5 μg) isolated from F9 cells was reverse transcribed in a total 20 μl volume reaction with 200 units of Superscript™ Reverse transcriptase II (Invitrogen Life Technologies) and oligo dT (12–18) primer (Invitrogen Life Technologies). The cDNA thus produced was diluted to 100 μl with diethyl pyrocarbonate/water, of which 2 μl was used in a PCR as follows. The PCR was performed using the following conditions: 94 °C for 30 s, 58 °C for 30 s, and 72 °C for 80 s, with a final extension at 72 °C for 10 min. *Taq* polymerase was from Invitrogen (catalog number 18038-042). The PCR products were subjected to 1% agarose gel electrophoresis. The gel images were stained with ethidium bromide and were recorded with a FluorChem 8800 system (Alpha Innotech, San Leandro, CA). Real-time PCR was performed using Bio-Rad iQ™ SYBR Green Supermix following the manufacturer's instructions, on a Bio-Rad MyiQ™ Single Color Real-time PCR Detection System. Primers used in this study are listed in Appendix 3.

3. Results

3.1. Comparison of the gene expression profiles in F9 Wt versus F9 RARγ$^{-/-}$ cell lines after treatment with RA plus a protein synthesis inhibitor, cycloheximide, for 6 h and after treatment with RA for 24 h

To identify the immediate, primary RARγ-regulated genes, F9 Wt and F9 RARγ$^{-/-}$ cells were treated with RA and the protein synthesis inhibitor, cycloheximide, for 6 h, and the gene expression profiles in the two cell lines were then compared using the U74Av2 affymetrix arrays. No untreated F9 Wt or F9 RARγ$^{-/-}$ samples were analyzed (Fig. 1). The rationale for this is that since RARγ is constitutively expressed in F9 cells, the primary target genes of RARγ should be transcriptionally activated by RA even in the absence of new protein synthesis. Thus, these transcripts can be detected in RA plus cycloheximide-treated F9 Wt cells, but not in the F9 cells which lack RARγ. A total number of 5885 probe sets which were flagged with presence in at least three chips were subjected to statistical analysis using GeneSpring V7 software. The resulting 94 genes exhibiting a twofold or greater net intensity ratio difference ($P \leq 0.05$, Welch's *t*-test) are shown (Table 1). These genes are putative RARγ primary target genes.

Wt	RARγ$^{-/-}$	Array type (Affymetrix)	#
1 μM RA+ CHM (6 h)	1 μM RA+ CHM (6h)	MG-U74Av2	3
1 μM RA (24h)	1 μM RA (24h)	MG-U74Av2	2
Control (24h)	Control (24h)	MG-430.2	3
1 μM RA (24h)	1 μM RA (24h)	MG-430.2	3

Fig. 1 – Design of microarray experiment. Four conditions were used to examine gene expression in F9 Wt and F9 RARγ$^{-/-}$ cells. A"#" indicates the number of times the microarray analysis was performed under each condition, starting with fresh cells. RA, all-*trans*-retinoic acid; CHM, cycloheximide.

The global gene expression patterns in F9 Wt and F9 RARγ$^{-/-}$ cells after a 24-h exposure to 1 μM RA were also compared on U74 Av2 arrays. The overall presence call was 6171/12,422 = 49.68%. After the Welch's *t*-test, 241 genes with *P*-values ≤ 0.05 were selected for further fold change analysis. The results from 66 genes exhibiting a twofold or greater net intensity ratio difference are shown (Table 2). These genes encode cell membrane proteins, cell–cell adhesion molecules, signal transducers, and surface tyrosine kinases involved in cell development. By comparing the 94 genes (6 h treatment with RA plus cycloheximide, Table 2) with those altered at 24 h after RA exposure (Table 2), we found that only 8 genes overlapped. These genes are the epithelial membrane protein (emp)-1, secreted frizzled-related sequence protein 2 (Sfrp2), alkaline phosphatase 2 (AKP2), Stmn2, solute carrier family 38 member 4 (Slc38a4), Slc27a2, and lectin–galactose binding soluble 3 (Lgals3). One obvious reason why the changes in most of the early response genes were not seen at the 24 h-RA treatment is that the kinetics of the transcriptional activation of the early *versus* late genes induced by RARγ are different.

To validate the microarray data, new F9 cell samples were treated with RA for 24 h to confirm the results. Several differentially expressed genes were selected for examination by semi-quantitative RT-PCR. In addition to the F9 Wt and RARγ$^{-/-}$ lines, F9 RARα$^{-/-}$ and RARβ$_2^{-/-}$ cell lines were also tested during the validation studies in order to determine if the genes were *specifically* regulated by RARγ. The mRNA expression of the different RAR isotypes α, β, and γ in each cell line was examined. The RARα$^{-/-}$, RARβ$_2^{-/-}$, and RARγ$^{-/-}$ cell lines were each established by homologous recombination with a targeting vector to their B domains [30–32]. Both alleles of the mutant RAR in each cell line contain the neomycin resistance gene, which disrupts the encoded RARα, RARβ$_2$, and RARγ transcripts and protein. Using primers specific for each isotype which span the neomycin resistance gene, the transcripts from the wild type allele and mutant allele were amplified. Since each of the mutant alleles contains the neomycin resistance gene, the mutant allele gives rise to a larger transcript than that from the wild type allele. RARα mRNA was detected in Wt, RARγ$^{-/-}$ and RARβ$_2^{-/-}$ cells, but not in F9 RARα$^{-/-}$ cells (Fig. 2A). The expression of RARβ$_2$ transcripts was strongly induced F9 Wt cells, F9 RARα$^{-/-}$, and RARγ$^{-/-}$ cells, but not in RA-treated RARβ$_2^{-/-}$ cells (Fig. 2A). RARγ mRNA could not be detected in F9 RARγ$^{-/-}$ cells, though RARγ mRNA was detected in F9 Wt, RARα$^{-/-}$ and RARβ$_2^{-/-}$ cells (Fig. 2A). Transcripts from the mutant RARγ (RARγ-NEO) were only detected in F9 RARγ$^{-/-}$, but not in F9 Wt, RARα$^{-/-}$ and RARβ$_2^{-/-}$ cells (Fig. 2A). Thus, the identities of the cell lines were confirmed (Fig. 2A).

Hoxa1, a known RARγ-regulated gene, was examined as a positive control. Hoxa1 mRNA levels increased after exposure

Table 1 – RARγ primary target genes identified using microarrays U74Av2

Affymetrix ID	Fold change[a,b]	Gene symbol	Gene title
103086_at	10.94	Hoxa5	Homeo box A5
102087_at	10.6	Hoxa3	Homeo box A3
97426_at	9.359	Emp1	Epithelial membrane protein 1
94813_at	7.189	Gas1	Growth arrest-specific 1
97379_at	5.973	Fbp2	Fructose bisphosphatase 2
104378_at	5.521	Pon2	Paraoxonase 2
104464_s_at	4.512	Kdelr3	KDEL (Lys-Asp-Glu-Leu) endoplasmic reticulum protein retention receptor 3
101861_at	4.397	Sgce	Sarcoglycan, epsilon
98320_at	4.226	Cyp26a1	Cytochrome P450, family 26, subfamily a, polypeptide 1
104406_at	4.208	Ptges	Prostaglandin E synthase
100914_at	4.204		Transcribed sequences
104580_at	4.168	Plcd	Phospholipase C, delta
93503_at	4.129	Sfrp2	Secreted frizzled-related sequence protein 2
95016_at	4.056	Nrp	Neuropilin
102649_s_at	4.051	Raet1a	Retinoic acid early transcript 1, alpha
103653_at	3.88	Mras	Muscle and microspikes RAS
99665_at	3.666	Satb1	Special AT-rich sequence binding protein 1
92502_at	3.588	Plagl1	Pleiomorphic adenoma gene-like 1
161013_f_at	3.435	4930422J18Rik	RIKEN cDNA 4930422J18 gene
161817_f_at	3.405	4930422J18Rik	RIKEN cDNA 4930422J18 gene
103761_at	3.403	Tcfcp2l1	Transcription factor CP2-like 1
104480_at	3.328	Dsg2	Desmoglein 2
104701_at	3.322	Bhlhb2	Basic helix-loop-helix domain containing, class B2
96662_at	3.195	Ppap2b	Phosphatidic acid phosphatase type 2B
99045_at	3.152	Eno2	Enolase 2, gamma neuronal
95474_at	3.087	F2r	Coagulation factor II (thrombin) receptor
104375_at	3.062	Spock2	Sparc/osteonectin, cwcv and kazal-like domains proteoglycan 2
92501_s_at	2.963	Plagl1	Pleiomorphic adenoma gene-like 1
93994_at	2.941	Chpt1	Choline phosphotransferase 1
92582_at	2.776	Slc1a5	Solute carrier family 1 (neutral amino acid transporter), member 5
94027_at	2.737		CDNA clone IMAGE:30033444, partial cds
97353_at	2.706	Dab2ip	Disabled homolog 2 (*Drosophila*) interacting protein
102712_at	2.706	Saa3	Serum amyloid A 3
100011_at	2.575	Klf3	Kruppel-like factor 3 (basic)
160961_at	2.57	Sipa1l2	Signal-induced proliferation-associated 1 like 2
102886_at	2.553	Gpc4	Glypican 4
92241_at	2.507	1110019L22Rik	RIKEN cDNA 1110019L22 gene
100410_at	2.47	C330027G06Rik	RIKEN cDNA C330027G06 gene
94418_at	2.467	Elovl6	ELOVL family member 6, elongation of long chain fatty acids (yeast)
98016_at	2.46	D3Wsu161e	DNA segment, Chr 3, Wayne State University 161, expressed
100528_at	2.45	Ube2h	Ubiquitin-conjugating enzyme E2H
95161_at	2.409	Ctdsp2	CTD (carboxy-terminal domain, RNA polymerase II, polypeptide A) small phosphatase 2
98535_at	2.402	Comt	Catechol-O-methyltransferase
93083_at	2.392	Anxa5	Annexin A5
160255_at	2.376	1110004P15Rik	RIKEN cDNA 1110004P15 gene
104576_at	2.371	Ski	Sloan-Kettering viral oncogene homolog
97509_f_at	2.37	Fgfr1	Fibroblast growth factor receptor 1
97138_at	2.369	9430077C05Rik	RIKEN cDNA 9430077C05 gene
92833_at	2.365	Hal	Histidine ammonia lyase
99994_at	2.335	Cidea	Cell death-inducing DNA fragmentation factor, alpha subunit-like effector A
97711_at	2.322	B430320C24Rik	RIKEN cDNA B430320C24 gene
160188_at	2.29	Nudt4	Nudix (nucleoside diphosphate linked moiety X)-type motif 4
104210_at	2.285	Itga3	Integrin alpha 3
103288_at	2.276	Nrip1	Nuclear receptor interacting protein 1
96207_at	2.264	Rbms1	RNA-binding motif, single stranded interacting protein 1
160393_at	2.167	Etnk1	Ethanolamine kinase 1
92796_at	2.162	Akp2	Alkaline phosphatase 2, liver
103614_at	2.128	Nfkb2	Nuclear factor of kappa light polypeptide gene enhancer in B-cells 2, p49/p100
92368_at	2.047	Ramp3	Receptor (calcitonin) activity modifying protein 3
100475_at	2.044	Trim25	B6-derived CD11 +ve dendritic cells cDNA, RIKEN full-length enriched library, clone: F730014H10 product: unclassifiable, full insert sequence

Table 1 (*Continued*)

Affymetrix ID	Fold change[a,b]	Gene symbol	Gene title
100962_at	2.039	Nab2	Ngfi-A binding protein 2
97452_at	2.038	H2afy	H2A histone family, member Y
160887_at	2.036	Hes1	Hairy and enhancer of split 1 (*Drosophila*)
94408_at	2.025	Nab1	Ngfi-A binding protein 1
103551_at	2	2810431N21Rik	RIKEN cDNA 2810431N21 gene
160546_at	0.487	Aldo3	Aldolase 3, C isoform
94829_at	0.466	1110020A09Rik	RIKEN cDNA 1110020A09 gene
92635_at	0.464	Tuba4	Tubulin, alpha 4
98109_at	0.462	Mrpl55	Mitochondrial ribosomal protein L55
103549_at	0.459	Nes	Nestin
93483_at	0.458	Hck	Hemopoietic cell kinase
98544_at	0.455	Guk1	Guanylate kinase 1
93543_f_at	0.452	Gstm1	glutathione S-transferase, mu 1
93836_at	0.439	Bnip3	BCL2/adenovirus E1B 19 kDa-interacting protein 1, NIP3
97995_at	0.431	Tcf7	Transcription factor 7, T-cell-specific
160495_at	0.423	Ahr	Aryl-hydrocarbon receptor
103581_at	0.407	Cte1	Cytosolic acyl-CoA thioesterase 1
94334_f_at	0.392	Ina	Internexin neuronal intermediate filament protein, alpha
103405_at	0.388	2610019A05Rik	RIKEN cDNA 2610019A05 gene
160085_at	0.384	Tst	Thiosulfate sulfurtransferase, mitochondrial
92786_at	0.359	Efhd1	EF hand domain containing 1
104652_at	0.349	Kcnk2	Potassium channel, subfamily K, member 2
94335_r_at	0.346	Ina	Internexin neuronal intermediate filament protein, alpha
95669_g_at	0.345	Stmn2	Stathmin-like 2
93680_at	0.344	Stk10	Serine/threonine kinase 10
99812_at	0.338	Capn3	Calpain 3
95670_at	0.296	Stmn2	Stathmin-like 2
95603_at	0.268	Gldc	Glycine decarboxylase
95706_at	0.267	Lgals3	Lectin, galactose binding, soluble 3
96244_at	0.239	Uchl1	Ubiquitin carboxy-terminal hydrolase L1
104286_at	0.183	Slc38a4	Solute carrier family 38, member 4
161068_at	0.12	3830422N12Rik	RIKEN cDNA 3830422N12 gene
100967_at	0.0994	Slc27a2	Solute carrier family 27 (fatty acid transporter), member 2
104544_at	0.0981	4930517K11Rik	RIKEN cDNA 4930517K11 gene

Wt and RARγ$^{-/-}$ F9 cells were treated for 6 h with 1 μg/ml cycloheximide and 1 μM RA. Only those genes with at least a 2.0-fold change in F9 Wt cells relative to F9 RARγ$^{-/-}$ cells in both sets of microarrays with P values ≤ 0.05 are shown. Fold change = F9 Wt/F9 RARγ$^{-/-}$.

[a] Average from three experiments.

[b] Some genes have multiple distinct probes on the GeneChip® resulting in different fold changes from different probes.

to RA in F9 Wt, RARα$^{-/-}$ and RARβ$_2$$^{-/-}$ cells, but the RA associated increase in Hoxa1 mRNA was greatly reduced in F9 RARγ$^{-/-}$ cells as compared to F9 Wt cells (Fig. 2B).

The nine genes chosen for validation by semi-quantitative RT-PCR analyses were FBP-2, Tie1, EMP1, EMP3, Sfrp2, Coch5B2, mOTT3, mFATP2 (Slc27a2), and Xlr3b (Fig. 2B). These genes were selected for validation because they exhibited relatively high fold changes in mRNA levels and/or interesting biological functions.

FBP-2 (fructose-1,6-bisphosphatase), via altering levels of F26P2 (fructose-2,6-bisphosphate), influences glucose and lipid metabolism and provides cooperative regulation of fuel metabolism [36]. F26P2 can in turn regulate transcription factors and certain key proteins (enzymes) of signaling and/or energy sensing [36]. For example, F26P2 can regulate the amount and/or phosphorylation state of transcription factors such as hepatic nuclear factor 1-alpha (HNF1α), peroxisome proliferator-activated receptor alpha (PPARα), and PPARγ co-activator 1beta (PGC1β), and the kinases Akt and AMP-activated protein kinase (AMPK) [36]. Fbp2 mRNA levels were 5.9 ± 2.0-fold and 3.5 ± 1.1-fold higher in F9 Wt cells than in F9 RARγ$^{-/-}$ cells cultured in the presence of RA plus cycloheximide for 6 h, and in the presence of RA for 24 h, respectively. Semi-quantitative RT-PCR confirmed that Fbp2 mRNA was present at higher levels in F9 Wt than in F9 RARγ$^{-/-}$ cells (Fig. 2B).

Tie1 is a member of the receptor tyrosine kinase family [37,38]. It is essential for the development and maintenance of vascular system and hematopoiesis [39]. *Tie1* mRNA levels were 25.1 ± 8.2-fold higher in F9 Wt than in F9 RARγ$^{-/-}$ cells cultured in the presence of RA for 24 h. Semi-quantitative RT-PCR confirmed that Tie1 mRNA levels were higher in F9 Wt cells than in F9 RARγ$^{-/-}$ cells (Fig. 2B).

Emp1 (epithelial membrane protein 1) and *Emp3* (epithelial membrane protein 3) are members of the peripheral myelin protein 22 (PMP22) family [40]. Emp1 mRNA levels were 9.4 ± 2.4-fold and 13.7 ± 3.5-fold higher in F9 Wt cells than in F9 RARγ$^{-/-}$ cells cultured in the presence of RA plus cycloheximide for 6 h, and cultured in the presence of RA for 24 h, respectively. Semi-quantitative RT-PCR confirmed that Emp1 and Emp3 transcripts are present at higher levels in F9 Wt than in F9 RARγ$^{-/-}$ cells (Fig. 2B).

Sfrp2 (secreted frizzled-related protein 2) is a secreted Wnt antagonist that directly interacts with the Wnt ligand to

Table 2 – Genes differentially expressed between F9 Wt and F9 RARγ$^{-/-}$ cells after RA treatment for 24 h, identified using U74Av2 microarrays

Affymetrix ID	Fold change[a,b]	Gene symbol	Gene title
99936_at	25.08	Tie1	Tyrosine kinase receptor 1
160943_at	15.3	Stag3	Stromal antigen 3
97426_at	13.86	Emp1	Epithelial membrane protein 1
93503_at	4.634	Sfrp2	Secreted frizzled-related sequence protein 2
101027_s_at	4.142	Pttg1	Pituitary tumor-transforming 1
103506_f_at	3.773	Dsc2	Desmocollin 2
104146_at	3.567	Rasip1	Ras interacting protein 1
97379_at	3.534	Fbp2	Fructose bisphosphatase 2
99669_at	3.532	Lgals1	Lectin, galactose binding, soluble 1
161482_f_at	3.427	Prph1	Peripherin 1
104580_at	3.385	Plcd	Phospholipase C, delta
100610_at	2.998	Capns1	Calpain, small subunit 1
95426_at	2.946	Echs1	Enoyl Coenzyme A hydratase, short chain, 1, mitochondrial
101358_at	2.885	Plcb3	Phospholipase C, beta 3
104746_at	2.821	Fkbp7	FK506 binding protein 7
160978_at	2.808	D630035O19Rik	RIKEN cDNA D630035O19 gene
96865_at	2.677	Marcks	Myristoylated alanine-rich protein kinase C substrate
98435_at	2.631	Adss	Adenylosuccinate synthetase, muscle
100828_at	2.325		–
160388_at	2.305	Sc4mol	Sterol-C4-methyl oxidase-like
160215_at	2.299	Aes	Amino-terminal enhancer of split
104232_at	2.289	Gjb3	Gap junction membrane channel protein beta 3
96016_at	2.27	2700094K13Rik	RIKEN cDNA 2700094K13 gene
102993_at	2.265	Ggta1	Glycoprotein galactosyltransferase alpha 1, 3
98535_at	2.247	Comt	Catechol-O-methyltransferase
92586_at	2.242	Glud	Glutamate dehydrogenase
99184_at	2.232	Csad	Cysteine sulfinic acid decarboxylase
101107_at	2.222	Calu	Calumenin
102926_at	2.193	Gfra3	Glial cell line derived neurotrophic factor family receptor alpha 3
93750_at	2.16	Gsn	Gelsolin
104673_at	2.137	Epha4	Eph receptor A4
103085_at	2.133	Hebp1	Heme binding protein 1
92607_at	2.103	Peg1	*Mus musculus* Peg1/MEST protein
93522_at	2.094	Rad9	RAD9 homolog (S. pombe)
95733_at	2.048	Slc29a1	Solute carrier family 29 (nucleoside transporters), member 1
97717_at	2.041	Tcf15	Transcription factor 15
92796_at	2.04	Akp2	Alkaline phosphatase 2, liver
96038_at	2.038	Rnase4	Ribonuclease, RNase A family 4
93373_at	2.023	Naglu	Alpha-*N*-acetylglucosaminidase (Sanfilippo disease IIIB)
103056_at	0.496	6230425C22Rik	RIKEN cDNA 6230425C22 gene
103423_at	0.495	Cyb561	Cytochrome *b*-561
93038_f_at	0.486	Anxa1	Annexin A1
95756_at	0.486	Ftsj3	FtsJ homolog 3 (*E. coli*)
100600_at	0.467	Cd24a	CD24a antigen
92306_at	0.465	Ott	Ovary testis transcribed
101030_at	0.426	Rhob	Ras homolog gene family, member B
102841_at	0.414		Similar to ribosomal protein L40 (LOC216818), mRNA
96151_at	0.407	Mocos	Molybdenum cofactor sulfurase
160236_at	0.383	9630044O09Rik	RIKEN cDNA 9630044O09 gene
95954_at	0.379	D7Ertd143e	DNA segment, Chr 7, ERATO Doi 143, expressed
93864_s_at	0.36	Enah	Enabled homolog (*Drosophila*)
95883_at	0.349	Phf17	PHD finger protein 17
104486_at	0.349	A2m	Alpha-2-macroglobulin
102344_s_at	0.345	Tcea3	Transcription elongation factor A (SII), 3
93680_at	0.343	Stk10	Serine/threonine kinase 10
102418_at	0.339	Tex19	Testis expressed gene 19
96704_at	0.339	Sfn	Stratifin
99577_at	0.33	Kitl	Kit ligand
104063_at	0.327	Srcasm	Src activating and signaling molecule
95670_at	0.308	Stmn2	Stathmin-like 2
99034_at	0.266	Irx3	Iroquois related homeobox 3 (*Drosophila*)
104338_r_at	0.25	1200008D14Rik	RIKEN cDNA 1200008D14 gene
93028_at	0.246	H19	H19 fetal liver mRNA
101883_at	0.212	Xlr3b	XLR-related protein, Mouse A12 mRNA

Table 2 (*Continued*)

Affymetrix ID	Fold change[a,b]	Gene symbol	Gene title
93294_at	0.211	Ctgf	Connective tissue growth factor
103317_at	0.189	Coch5B2	Coagulation factor C homolog (Limus polyphemus) cds = (68,1726)
100967_at	0.189	Slc27a2	Solute carrier family 27 (fatty acid transporter), member 2
104126_at	0.188	Cstf2t	Cleavage stimulation factor, 3′ pre-RNA subunit 2, tau
161081_at	0.158	Cpeb2	Cytoplasmic polyadenylation element binding protein 2
104286_at	0.106	Slc38a4	Solute carrier family 38, member 4
93013_at	0.0853	Idb2	Inhibitor of DNA binding 2
95706_at	0.0819	Lgals3	Lectin, galactose binding, soluble 3

Only those genes with at least a twofold change in F9 Wt cells relative to F9 RARγ$^{-/-}$ cells with *P* values ≤ 0.05 are shown. Fold change = F9 Wt/F9 RARγ$^{-/-}$.

[a] Average from two experiments.

[b] Some genes have multiple distinct probes on the GeneChip® resulting in different fold changes from different probes.

inhibit Wnt signaling [41]. Sfrp2 is required for anteroposterior (AP) axis elongation and somitogenesis in the thoracic region during mouse embryogenesis. *Sfrp2* mRNA levels were 4.1 ± 1.7-fold higher in F9 Wt than in F9 RARγ$^{-/-}$ cells cultured in the presence of RA plus cycloheximide for 6 h, and 4.6 ± 2.0-fold cultured in the presence of RA for 24 h, respectively. Semi-quantitative RT-PCR confirmed that *Sfrp2* mRNA levels are higher in F9 Wt cells than in F9 RARγ$^{-/-}$ cells (Fig. 2B).

Coch5B2 encodes a protein with regions highly homologous to the collagen-binding type A domains of von Willebrand factor [42]. Coch5B2 is highly expressed in fetal inner ear structures, the cochlea, and the vestibule [43]. Mutations in Coch5B2 cause DFNA9, a human non-syndromic deafness with vestibular dysfunction [44,45]. Coch 5B2 mRNA levels were 5.3 ± 1.4-fold higher in the F9 RARγ$^{-/-}$ cells than in F9 Wt cells cultured in the presence of RA for 24 h, and this was confirmed by semi-quantitative RT-PCR (Fig. 2B).

OTT3 is an X-linked gene expressed in testis and spermatogonia, but not in somatic tissues [46]. A role for OTT3 in splicing regulation has been demonstrated [47]. Ott3 mRNA levels were 2.2 ± 0.7-fold higher in F9 RARγ$^{-/-}$ cells than in F9 Wt cells cultured in the presence of RA for 24 h, and this was validated by semi-quantitative RT-PCR (Fig. 2B).

Slc27a2 (solute carrier family 27 (fatty acid transporter), member 2) belongs to the long chain fatty acid transporter (FATP) family. These proteins facilitate fatty acid uptake from the medium [48]. *Slc27a2* mRNA levels were 2.2 ± 0.3-fold higher in F9 RARγ$^{-/-}$ cells than in F9 Wt cells cultured in the presence of RA for 24 h, and this was confirmed by semi-quantitative RT-PCR (Fig. 2B).

Xlr3b (X-linked lymphocyte regulated, 3b) is an X-linked, maternally expressed, imprinted gene [49] which may mediate X-linked imprinting effects on cognitive processes [50,51]. Xlr3b mRNA levels were 4.7 ± 1.3-fold higher in F9 RARγ$^{-/-}$ cells than in F9 Wt cells cultured in the presence of RA for 24 h and semi-quantitative RT-PCR confirmed that Xlr3b mRNA levels are higher in F9 RARγ$^{-/-}$ cells than in F9 Wt cells (Fig. 2B).

The mRNA levels of FBP-2, Tie1, EMP1, EMP3 and Sfrp2 were lower in F9 RARγ$^{-/-}$ cells than in F9 Wt cells, but these transcripts were not expressed at lower levels in F9 RARα$^{-/-}$ and RARβ$_2$$^{-/-}$ cells, either in the presence or absence of RA. Thus, these genes represent specific RARγ target genes. In contrast, Coch5B2, mOTT3, Slc27a2, and Xlr3b transcripts were expressed at higher levels in F9 RARγ$^{-/-}$ cells than in Wt, RARα$^{-/-}$ (with the exception of Slc27a2), and RARβ$_2$$^{-/-}$ cells. Coch5B2, Xlr3b and mOTT3 transcripts, therefore, are specifically increased in F9 RARγ$^{-/-}$ cells (Fig. 2B). A list of these genes is in the GEO database (www.ncbi.nlm.nih.gov/geo, accession # GSE8431).

3.2. Comparison of the gene expression profiles associated with F9 Wt and F9 RARγ$^{-/-}$ cells cultured in the absence versus presence of RA

The initial microarray analyses we performed identified the genes that are differentially expressed between RA-treated F9 Wt and RA-treated F9 RARγ$^{-/-}$ cells at 6 h and 24 h, but no control (untreated) F9 Wt or F9 RARγ$^{-/-}$ samples were analyzed (Fig. 1). Thus, the genes identified in these initial studies also included a subset of genes that were not responsive to RA. In order to identify additional RA-responsive genes and to incorporate a larger fraction of the mouse genome into our survey of RARγ-regulated genes, we performed another microarray analysis utilizing Affymetrix MG-430.2 gene chips, which contain 45,037 transcripts representing 34,000 well-substantiated mouse genes.F9 Wt and F9 RARγ$^{-/-}$ cells were treated with either 1 μM RA or vehicle (ethanol) for 24 h. The gene expression profiles of RA-treated F9 Wt cells, vehicle-treated (control) F9 Wt cells, RA-treated F9 RARγ$^{-/-}$ cells, and vehicle-treated (control) F9 RARγ$^{-/-}$ cells were then compared using MG-430.2 gene chips. The genes that were differentially expressed between F9 Wt cells and F9 RARγ$^{-/-}$ cells in the presence or absence of RA were identified. Since a protein synthesis inhibitor was not used in this set of experiments, both primary and secondary RARγ-dependent RA-response genes were identified.In order to identify the subset of RARγ-regulated, RA-responsive genes, a strategy involving multiple two-condition comparisons was employed (Fig. 3). Genes were only considered differentially expressed between the two conditions if they exhibited at least a twofold difference in expression with a *P* value of less than 0.05 (Welch's *t*-test). Genes were defined as RA-responsive genes if they exhibited at least a twofold difference from the control (no RA) condition ($P \leq 0.05$). For the analysis with MG-430.2 chips, all of the genes with a "Present" call in at least three chips were selected and were subjected to statistical analysis for two condition comparisons using GeneSpring v7.0. The overall presence call (# of genes with a Present call/total # of probe sets on the array) for those samples was 23,329/45,037 = 51.78%. For filtering the data for

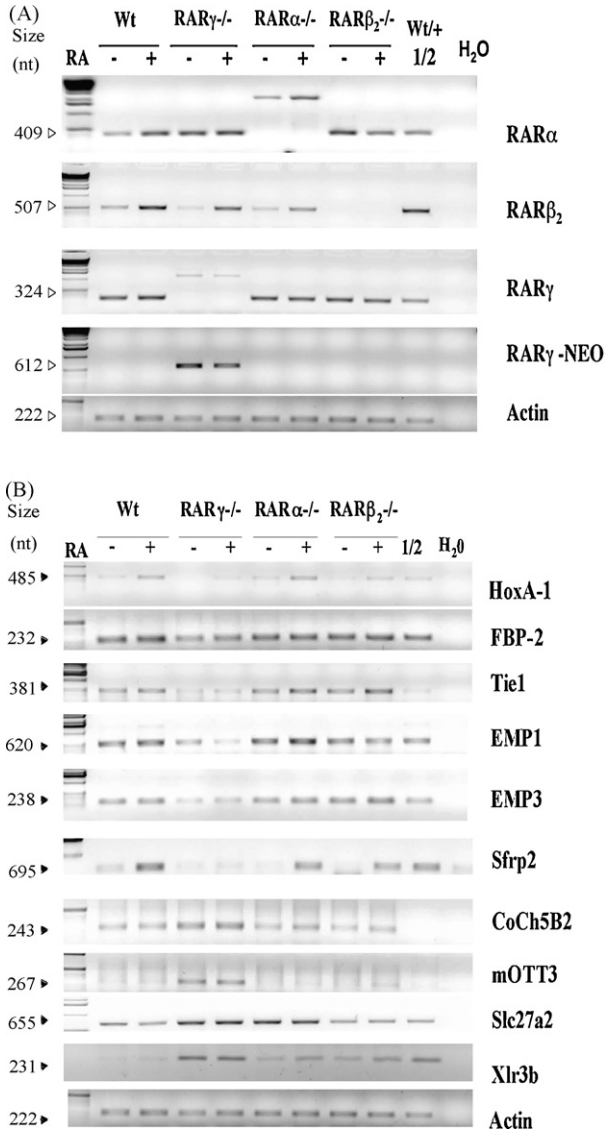

Fig. 2 – Semi-quantitative RT-PCR analyses of selected genes, FBP-2, Tie1, EMP1, EMP3, Sfrp2, Coch5B2, mOTT3, mFATP2, and Xlr3b, in F9 Wt, RARγ$^{-/-}$, RARα$^{-/-}$ and RARβ$_2$$^{-/-}$ cell lines in response to RA. A and B, total RNA was extracted from the F9 Wt, RAR γ$^{-/-}$, RARα$^{-/-}$, RARβ$_2$$^{-/-}$ cells cultured in the presence or absence of 1 μM RA for 24 h. An equivalent amount of RNA (5 μg) was subjected to RT-PCR with oligonucleotide primers specific for the indicated genes. The PCRs were stopped between the 22nd and 32nd cycles depending on the gene being tested to ensure linear amplification ranges. PCR-amplified products were electrophoresed in 1% agarose gels and the products were stained with ethidium bromide. The 1:2 dilution of cDNA from RA-treated F9 Wt or RA-treated F9 RARγ$^{-/-}$ samples was used to indicate the linear amplification ranges for genes which showed increased mRNA levels in RARγ$^{-/-}$ cells or decreased levels in RARγ$^{-/-}$ cells, respectively. The sizes of the amplified bands are indicated on the left. These assays were repeated using three different RNA preparations, and similar results were obtained.

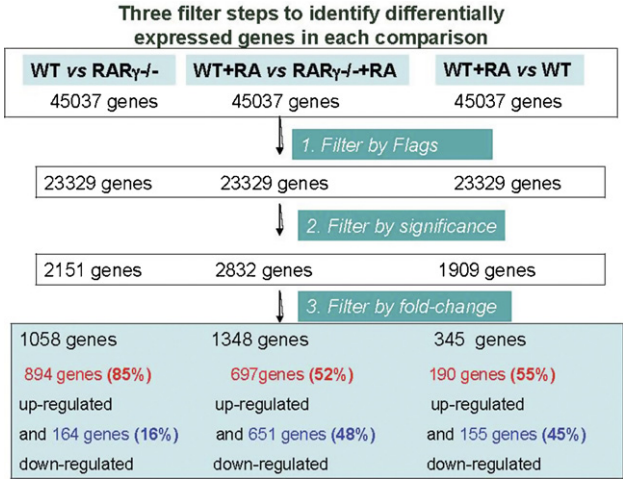

Fig. 3 – An overview of the strategy to select differentially expressed genes. Beginning with all Affymetrix IDs on the MG-430 2.0 GeneChip (45,037 genes), the first filter selected the genes with a "Present" call in at least three microarrays. The second step filtered out statistically insignificant means based on the Welch's *t*-test. The third step filtered out genes with less than a twofold difference in expression between the two conditions.

significant changes, the parameteric Welch's *t*-test was performed individually for each of the following pair comparisons: vehicle-treated (control) F9 Wt cells *versus* vehicle-treated (control) F9 RARγ$^{-/-}$ cells (Wt *versus* RARγ$^{-/-}$); RA-treated Wt cells *versus* RA-treated RARγ$^{-/-}$ cells (Wt + RA *versus* RARγ$^{-/-}$ + RA); RA-treated Wt cells *versus* vehicle-treated control Wt cells (Wt + RA *versus* Wt); resulting in 2151 genes, 2832 genes, and 1909 genes that had statistically significant *P* values ≤ 0.05, respectively. Genes with statistically significant differences in expression ($P < 0.05$) were then further subjected to a fold change filter application, resulting in 1058 genes (Wt *versus* RARγ$^{-/-}$), 1348 genes (Wt + RA *versus* RARγ$^{-/-}$+RA), and 345 genes (Wt + RA *versus* Wt), respectively, with a differential expression of at least twofold for each pair comparison (Fig. 3).

3.3. *Distinctive expression profiles associated with the F9 Wt and F9 RARγ$^{-/-}$ cell lines cultured in the absence of RA*

There were a total of 1058 probe sets differentially expressed by at least twofold between the vehicle-treated (control) F9 Wt and vehicle-treated control F9 RARγ$^{-/-}$ cells at 24 h (Fig. 3). This indicates a fundamental difference in the gene expression profiles between the two cell types in the *absence* of RA. The differentially expressed genes with the highest fold changes are shown (Tables 3A and 3B). After a 24 h-RA treatment, a total of 1348 probe sets exhibited at least a twofold difference in expression between the RA-treated Wt and RA-treated RARγ$^{-/-}$ F9 cells (Fig. 3), and the differentially expressed genes with the highest fold changes are listed (Tables 4A and 4B).

The mRNA levels of these genes were greater than 10-fold higher in F9 Wt cells than in F9 RARγ$^{-/-}$ cells cultured in the

Table 3A – Top 53 genes with at least twofold higher expression in F9 Wt cells relative to F9 RARγ$^{-/-}$ cells at 24 h in the absence of RA. Fold change = WT/RARγ$^{-/-}$

Affymetrix ID	Fold change[a,b]	Gene symbol	Gene title
1431094_at	43.31	Rtl1	Retrotransposon-like 1
1456250_x_at	42.39	Tgfbi	BB533460 RIKEN full-length enriched, 0 day neonate lung *Mus musculus* cDNA clone E030030E06 3′ similar to L19932 Mouse (beta ig-h3) mRNA, mRNA sequence
1417426_at	38.65	Prg1	Proteoglycan 1, secretory granule
1452183_a_at	38.62	Gtl2	GTL2, imprinted maternally expressed untranslated mRNA
1448123_s_at	34.09	H2-Ab1	Histocompatibility 2, class II antigen A, beta 1
1422865_at	31.5	Spp1	Secreted phosphoprotein 1
1439380_x_at	29.61	Gtl2	BB093563 RIKEN full-length enriched, 12 days embryo, embryonic body between diaphragm region and neck *Mus musculus* cDNA clone 9430042P15 3′ similar to Y13832 *Mus musculus* mRNA for GT12 protein, mRNA sequence
1415871_at	27.87	H2-Ab1	Histocompatibility 2, class II antigen A, beta 1
1448926_at	27.49	Hoxa5	Homeo box A5
1441075_at	25.77	LOC329416	Nitric oxide synthase trafficker
1418215_at	25.05	Mep1b	Meprin 1 beta
1432159_a_at	24.87	Il2	Interleukin 2
1452905_at	24.52	Gtl2	GTL2, imprinted maternally expressed untranslated mRNA
1455626_at	23.25	Hoxa9	Homeo box A9
1425109_at	20.16	Slc44a3	Solute carrier family 44, member 3
1422864_at	19.68	Spp1	Secreted phosphoprotein 1
1423294_at	18.68	Mest	Transcribed sequence with moderate similarity to protein sp: Q9UBF2 (*H. sapiens*) CPG2_HUMAN Coatomer gamma-2 subunit
1435989_x_at	18.51	Krt2-8	Keratin complex 2, basic, gene 8
1427580_a_at	18.48	Rian	15 days embryo head cDNA, RIKEN full-length enriched library, clone: D930050K13 product: unclassifiable, full insert sequence
1426990_at	18.39	Cubn	Cubilin (intrinsic factor-cobalamin receptor)
1429273_at	18.02	Bmper	BMP-binding endothelial regulator
1452400_a_at	17.57	Hoxa11s	Homeo box A11, opposite strand transcript
1419537_at	17.39	Ctsd	Cathepsin D
1460550_at	16.3	BC051083	cDNA sequence BC051083
1417787_at	16.24	Prnd	Prion protein dublet
1451332_at	16.03	Zfp521	Zinc finger protein 521; synonyms: Evi3, B930086A16Rik; isoform 2 is encoded by transcript variant 2; ecotropic viral integration site 3; *Mus musculus* zinc finger protein 521 (Zfp521), transcript variant 2, mRNA.
1448804_at	15.79	Cyp11a1	Cytochrome P450, family 11, subfamily a, polypeptide 1
1430637_at	15.68	2210016H18Rik	Adult male stomach cDNA, RIKEN full-length enriched library, clone: 2210016H18 product: hypothetical protein, full insert sequence
1418713_at	15.56	Pcbd1	Pterin 4 alpha carbinolamine de hydratase/dimerization cofactor of hepatocyte nuclear factor 1 alpha (TCF1) 1
1431475_a_at	15.11	Hoxa10	Homeo box A10
1458232_at	15.1	Dkk1	dickkopf homolog 1 (Xenopus laevis)
1434647_at	14.92	AU040377	Expressed sequence AU040377
1427433_s_at	14.79	5730446D14Rik	RIKEN cDNA 5730446D14 gene
1428781_at	13.99	1110014F24Rik	RIKEN cDNA 1110014F24 gene
1451687_a_at	12.91	Tcf2	Transcription factor 2
1451191_at	12.51	Crabp1	Cellular retinoic acid binding protein I
1418672_at	12.46	Lrrc1	Leucine rich repeat containing 1
1418187_at	12.46	Ramp2	Receptor (calcitonin) activity modifying protein 2
1429693_at	12.41	Dab2	Disabled homolog 2 (*Drosophila*)
1424393_s_at	12.14	Syt11	Synaptotagmin XI
1453782_at	11.99	3021401C12Rik	RIKEN cDNA 0610012A05 gene
1443696_s_at	11.95	Habp2	Hyaluronic acid binding protein 2

Table 3A (*Continued*)

Affymetrix ID	Fold change[a,b]	Gene symbol	Gene title
1433670_at	11.65	Emp2	Epithelial membrane protein 2
1450555_at	11.56	Il2	Interleukin 2
1460722_at	11.52	Soat2	Sterol-O-acyltransferase 2
1449568_at	11.4	Klb	Klotho beta
1440878_at	11.38	Runx1	Runt related transcription factor 1
1420360_at	11.05	Dkk1	Dickkopf homolog 1 (Xenopus laevis)
1420565_at	10.88	Hoxa1	Homeo box A1
1417828_at	10.62	Aqp8	Aquaporin 8
1449088_at	10.47	Eef2	Eukaryotic translation elongation factor 2
1456733_x_at	10.36	Serpinh1	BB329489 RIKEN full-length enriched, 4 days neonate thymus *Mus musculus* cDNA clone B630008L19 3′, mRNA sequence
1417920_at	10.22	Creb1	CAMP-responsive element binding protein 1
1438558_x_at	9.989	Foxq1	Forkhead box Q1

[a] Average from three experiments.
[b] Some genes have multiple distinct probes on the GeneChip® resulting in different fold changes from different probes.

Table 3B – Top 50 genes with at least twofold lower expression in F9 Wt cells relative to F9 RARγ$^{-/-}$ cells after 24 h in the absence of RA. Fold change = WT/RARγ$^{-/-}$

Affymetrix ID	Fold change[a,b]	Gene symbol	Gene title
1436796_at	0.307	1110061A14Rik	Matrin 3
1422557_s_at	0.305	Mt1	Metallothionein 1
1450292_a_at	0.305	Ap3b1	Adaptor-related protein complex 3, beta 1 subunit
1448991_a_at	0.302	Ina	Internexin neuronal intermediate filament protein, alpha
1450417_a_at	0.301	Rps20	Ribosomal protein S20
1457195_at	0.299	Plekhm1	cDNA sequence BC038943
1424490_at	0.292	Atp5o	ATP synthase, H+ transporting, mitochondrial F1 complex, O subunit
1454681_at	0.288	2210008M09Rik	cDNA sequence BC031468
1429490_at	0.286	Rif1	Rap1 interacting factor 1 homolog (yeast)
1417751_at	0.285	Mapk7	Mitogen activated protein kinase 7
1418994_at	0.283	2410116G06Rik	RIKEN cDNA 2410116G06 gene
1437311_at	0.279	A930034L06Rik	RIKEN cDNA A930034L06 gene
1425415_a_at	0.255	Slc1a1	Solute carrier family 1 (neuronal/epithelial high affinity glutamate transporter, system Xag), member 1
1416149_at	0.252	Akt2	Thymoma viral proto-oncogene 2
1436619_at	0.251		H3077A05-3 NIA Mouse 15K cDNA Clone Set *Mus musculus* cDNA clone H3077A05 3′, mRNA sequence
1460204_at	0.251	Tsc2	Tuberous sclerosis 2
1427046_at	0.246	1810073N04Rik	RIKEN cDNA 1810073N04 gene
1423281_at	0.246	Stmn2	Stathmin-like 2
1440997_at	0.246	9930033H14Rik	RIKEN cDNA 9930033H14 gene
1455688_at	0.245	AI838577	Adult male urinary bladder cDNA, RIKEN full-length enriched library, clone: 9530036D08 product: unknown EST, full insert sequence
1439880_at	0.238	D630023F18Rik	Transcribed sequences
1453219_a_at	0.231	L1td1	LINE-1 type transposase domain containing 1
1425035_s_at	0.23	Dnmt3l	DNA (cytosine-5-)-methyltransferase 3-like
1421299_a_at	0.229	Lef1	Lymphoid enhancer binding factor 1
1423280_at	0.226	Stmn2	Stathmin-like 2
1458599_at	0.223		Transcribed sequences
1443858_at	0.218	Trim34	RIKEN cDNA 9230105E10 gene
1448299_at	0.217	Slc1a1	Solute carrier family 1 (neuronal/epithelial high affinity glutamate transporter, system Xag), member 1
1436388_a_at	0.213	3830406C13Rik	RIKEN cDNA 3830406C13 gene
1425926_a_at	0.199	Otx2	Orthodenticle homolog 2 (*Drosophila*)
1460386_a_at	0.197	Slc1a1	Solute carrier family 1 (neuronal/epithelial high affinity glutamate transporter, system Xag), member 1
1418825_at	0.195	Psmd11	Proteasome (prosome, macropain) 26S subunit, non-ATPase, 11

Table 3B (*Continued*)

Affymetrix ID	Fold change[a,b]	Gene symbol	Gene title
1433789_at	0.158	Rnu17d	18 days pregnant adult female placenta and extra embryonic tissue cDNA, RIKEN full-length enriched library, clone: 3830421G02 product: unknown EST, full insert sequence
1445271_at	0.151	9230105E10Rik	RIKEN cDNA 9230105E10 gene
1445617_at	0.15		Transcribed sequences
1439207_at	0.149		Similar to paraneoplastic antigen like 5; paraneoplastic antigen family 5 (LOC386569), mRNA
1423327_at	0.133	D730048I06Rik	RIKEN cDNA D730048I06 gene
1429203_at	0.131	2410076I21Rik	RIKEN cDNA 2410076I21 gene
1433792_at	0.131	AW491344	Transcribed sequence with weak similarity to protein ref: NP_113662.1 (*H. sapiens*) hypothetical protein DKFZp761G1913 [*Homo sapiens*]
1448558_a_at	0.118	Pla2g4a	Phospholipase A2, group IVA (cytosolic, calcium-dependent)
1422617_at	0.102	Top1	Topoisomerase (DNA) I
1429701_at	0.101	2410003J06Rik	RIKEN cDNA 2410003J06 gene
1434739_at	0.0949	3830422N12Rik	RIKEN cDNA 3830422N12 gene
1453544_at	0.0876	4933424F23Rik	RIKEN cDNA 4933424F23 gene
1449625_at	0.0707		Transcribed sequence with weak similarity to protein ref: NP_570953.1 (*M. musculus*) CAMP [*Mus musculus*]
1419241_a_at	0.0671	Aire	Autoimmune regulator (autoimmune polyendocrinopathy candidiasis ectodermal dystrophy)
1420357_s_at	0.0663	Fndc6	Fibronectin type III domain containing 6
1447021_at	0.0447		CDNA clone MGC: 61032 IMAGE: 30024827, complete cds
1448889_at	0.0344	Slc38a4	Solute carrier family 38, member 4
1428111_at	0.028	Slc38a4	Solute carrier family 38, member 4
1423523_at	0.0225	Aass	Aminoadipate-semialdehyde synthase

[a] Average from three experiments.
[b] Some genes have multiple distinct probes on the GeneChip® resulting in different fold changes from different probes.

Table 4A – Top 50 genes with at least twofold higher expression in RA-treated Wt F9 cells relative to RA-treated RARγ$^{-/-}$ cells at 24 h. Fold change = F9 Wt/F9 RARγ$^{-/-}$

Affymetrix ID	Fold change[a,b]	Gene symbol	Gene title
1455498_at	122.6		Transcribed sequence with weak similarity to protein pir:A43932 (*H. sapiens*) A43932 mucin 2 precursor, intestinal—human
1451332_at	71.76	Zfp521	Zinc finger protein 521; synonyms: Evi3, B930086A16Rik; isoform 2 is encoded by transcript variant 2; ecotropic viral integration site 3; *Mus musculus* zinc finger protein 521 (Zfp521), transcript variant 2, mRNA
1441075_at	51	LOC329416	Nitric oxide synthase trafficker
1452183_a_at	48.69	Gtl2	GTL2, imprinted maternally expressed untranslated mRNA
1428055_at	47.37		15 days embryo head cDNA, RIKEN full-length enriched library, clone: D930050K13 product: unclassifiable, full insert sequence
1417426_at	35.01	Prg1	Proteoglycan 1, secretory granule
1452905_at	34.73	Gtl2	GTL2, imprinted maternally expressed untranslated mRNA
1432159_a_at	31.56	Il2	Interleukin 2
1450555_at	25.66	Il2	Interleukin 2
1423294_at	25.26	Mest	Transcribed sequence with moderate similarity to protein sp: Q9UBF2 (*H. sapiens*) CPG2_HUMAN Coatomer gamma-2 subunit
1423023_at	24.61	Sfrp5	Secreted frizzled-related sequence protein 5
1439380_x_at	24.04	Gtl2	BB093563 RIKEN full-length enriched, 12 days embryo, embryonic body between diaphragm region and neck *Mus musculus* cDNA clone 9430042P15 3′ similar to Y13832 *Mus musculus* mRNA for GT12 protein, mRNA sequence
1415871_at	24	H2-Ab1	Histocompatibility 2, class II antigen A, beta 1
1460550_at	23.48	BC051083	cDNA sequence BC051083
1429273_at	23.48	Bmper	BMP-binding endothelial regulator
1448926_at	22.68	Hoxa5	Homeo box A5
1437347_at	21.85	Ednrb	Endothelin receptor type B

Table 4A (*Continued*)

Affymetrix ID	Fold change[a,b]	Gene symbol	Gene title
1430637_at	20.7	2210016H18Rik	Adult male stomach cDNA, RIKEN full-length enriched library, clone: 2210016H18 product: hypothetical protein, full insert sequence
1421952_at	19.86	Capn6	Calpain 6
1421224_a_at	19.8	Tcf2	Transcription factor 2
1456250_x_at	19.4	Tgfbi	BB533460 RIKEN full-length enriched, 0 day neonate lung *Mus musculus* cDNA clone E030030E06 3′ similar to L19932 Mouse (beta ig-h3) mRNA, mRNA sequence
1436172_at	19.3		Adult male testis cDNA, RIKEN full-length enriched library, clone: 4921508F21 product: similar to HISTOCOMPATIBILITY 2, CLASS II ANTIGEN E BETA [*Mus musculus*], full insert sequence
1455626_at	17.4	Hoxa9	Homeo box A9
1426758_s_at	17.38	Gtl2	GTL2, imprinted maternally expressed untranslated mRNA
1422866_at	17.33	Col13a1	Procollagen, type XIII, alpha 1
1436713_s_at	16.96		L0922F05-3 NIA Mouse Newborn Kidney cDNA Library (Long) *Mus musculus* cDNA clone NIA: L0922F05 IMAGE: 30002176 3′, mRNA sequence
1425273_s_at	15.6	Emp2	Epithelial membrane protein 2
1440878_at	15.18	Runx1	Runt-related transcription factor 1
1459742_at	14.46		BB800744 RIKEN full-length enriched, 15 days embryo brain *Mus musculus* cDNA clone G630032A08 3′, mRNA sequence
1420603_s_at	14.36	Sgk3	Serum/glucocorticoid regulated kinase 3
1422865_at	12.97	Spp1	Secreted phosphoprotein 1
1450759_at	12.89	BC019943	CDNA sequence BC019943
1433428_x_at	12.67	Tgm2	Transglutaminase 2, C polypeptide
1416855_at	12.61	Gas1	BB550400 RIKEN full-length enriched, 2 days pregnant adult female oviduct *Mus musculus* cDNA clone E230022A16 3′ similar to X65128 *M. musculus* gas1 mRNA, mRNA sequence
1448123_s_at	12.58	H2-Ab1	Histocompatibility 2, class II antigen A, beta 1
1421917_at	12.28	Pdgfra	Platelet-derived growth factor receptor, alpha polypeptide
1452400_a_at	12.15	Hoxa11s	Homeo box A11, opposite strand transcript
1438558_x_at	11.59	Foxq1	Forkhead box Q1
1432673_at	11.11	2300010F08Rik	12 days embryo embryonic body between diaphragm region and neck cDNA, RIKEN full-length enriched library, clone: 9430087B15 product: unclassifiable, full insert sequence
1450624_at	10.81	Surf4	Surfeit gene 4
1429177_x_at	10.6	Mafg	V-maf musculoaponeurotic fibrosarcoma oncogene family, protein G (avian)
1423805_at	10.3	Dab2	Disabled homolog 2 (*Drosophila*)
1424649_a_at	10.22	Tspan8	Tetraspanin 8
1449088_at	10.12	Eef2	Eukaryotic translation elongation factor 2
1429693_at	9.983	Dab2	Disabled homolog 2 (*Drosophila*)
1451191_at	9.949	Crabp1	Cellular retinoic acid binding protein I
1433615_at	9.937	B930062P21Rik	RIKEN cDNA B930062P21 gene
1417787_at	9.648	Prnd	Prion protein dublet
1429310_at	9.583	Flrt3	Fibronectin leucine rich transmembrane protein 3
1426341_at	9.02	Slc1a3	Solute carrier family 1 (glial high affinity glutamate transporter), member 3

[a] Average from three experiments.
[b] Some genes have multiple distinct probes on the GeneChip® resulting in different fold changes from different probes.

absence of RA: retrotransposon-like 1, meprin 1 beta, nitric oxide synthase trafficker, runt-related transcription factor 1 (Runx-1), transcription factor 2, Zfp521 (Evi3), GTL2 (the imprinted maternally expressed untranslated mRNA), prg (proteoglycan, secretory granule), tex13 (testis expressed gene 13), Mest, Tgfbi, Bmper (BMP-binding endothelial regulator), Dab2, Col13a1, BMP6, Foxq1, aquaporin 8, EMP2 and Amot (angiomotin). Since some of these genes, such as Dab2, BMP6, Foxq1, Hoxa1, and Col13a1, play critical roles in F9 endoderm differentiation, the lower expression of these genes in the F9 RARγ$^{-/-}$ cells relative to F9 Wt cells could reflect a reduced differentiation potential of the F9 RARγ$^{-/-}$ cells. The F9 RARγ$^{-/-}$ cells have been shown to exhibit reduced RA associated endoderm differentiation [30].

Genes exhibiting greater than fivefold higher mRNA levels in F9 RARγ$^{-/-}$ cells than in F9 Wt cells in the absence of RA included Aass (aminoadipate-semialdehyde synthase), Slc38a4, Xlr3a, Aire, RIKEN cDNA 3830422N12 gene, RIKEN cDNA 4933424F23 gene, topoisomerase (DNA) I, Pla2g4a (Phospholipase A2, group IVA (cytosolic, calcium-dependent)), Ifi1 (Proteasome (prosome, macropain) 26S subunit, non-ATPase, 11), Slc1a1, and Otx2.

Table 4B – Top 50 genes with at least twofold lower expression in RA-treated Wt F9 cells relative to RA-treated RARγ$^{-/-}$ cells at 24 h. Fold change = F9 Wt/F9 RARγ$^{-/-}$.

Affymetrix ID	Fold change[a,b]	Gene symbol	Gene title
1419227_at	0.195	Cct6b	Chaperonin subunit 6b (zeta)
1424531_a_at	0.191	Tcea3	Transcription elongation factor A (SII), 3
1449005_at	0.188	Itgav	Integrin alpha V
1436657_at	0.187		LOC380738 (LOC380738), mRNA
1455015_at	0.187	4933431N12Rik	RIKEN cDNA 4933431N12 gene
1452384_at	0.187	Enpp3	Ectonucleotide pyrophosphatase/phosphodiesterase 3
1455881_at	0.186	2610524G09Rik	RIKEN cDNA 2610524G09 gene
1416626_at	0.185	Pla2g1b	Phospholipase A2, group IB, pancreas
1441971_at	0.184		Transcribed sequences
1436677_at	0.184	1810032O08Rik	Sialyltransferase 7 ((alpha-*N*-acetylneuraminyl 2,3-beta-galactosyl-1,3)-*N*-acetyl galactosaminde alpha-2, 6-sialyltransferase) B
1416953_at	0.183	Ctgf	Connective tissue growth factor
1426808_at	0.181	Lgals3	Lectin, galactose binding, soluble 3
1450989_at	0.18	Tdgf1	Teratocarcinoma-derived growth factor
1428942_at	0.178	Mt2	Metallothionein 2
1434719_at	0.175	A2m	Alpha-2-macroglobulin
1434094_at	0.162	6330530A05Rik	RIKEN cDNA 6330530A05 gene
1423281_at	0.161	Stmn2	Stathmin-like 2
1453219_a_at	0.149	L1td1	LINE-1 type transposase domain containing 1
1425035_s_at	0.144	Dnmt3l	DNA (cytosine-5-)-methyltransferase 3-like
1431633_x_at	0.142	4930526L06Rik	Adult male testis cDNA, RIKEN full-length enriched library, clone: 4930526L06 product: unknown EST, full insert sequence
1423280_at	0.137	Stmn2	Stathmin-like 2
1439207_at	0.135		Similar to paraneoplastic antigen like 5; paraneoplastic antigen family 5 (LOC386569), mRNA
1433789_at	0.13	Rnu17d	18 days pregnant adult female placenta and extra embryonic tissue cDNA, RIKEN full-length enriched library, clone: 3830421G02 product: unknown EST, full insert sequence
1450943_at	0.128	Ndufa11	NADH dehydrogenase (ubiquinone) 1 alpha subcomplex 11
1439746_at	0.126	C130085G02Rik	RIKEN cDNA C130085G02 gene
1423327_at	0.122	D730048I06Rik	RIKEN cDNA D730048I06 gene
1423378_at	0.115	Adam23	A disintegrin and metalloprotease domain 23
1436388_a_at	0.114	3830406C13Rik	RIKEN cDNA 3830406C13 gene
1417156_at	0.104	Krt19	Keratin 19
1437786_at	0.095	C80008	Transcribed sequences
1453874_at	0.0878	4933401B06Rik	RIKEN cDNA 4933401B06 gene
1456035_at	0.0827		Transcribed sequences
1425926_a_at	0.0799	Otx2	Orthodenticle homolog 2 (*Drosophila*)
1450177_at	0.0773	Ngfr	Nerve growth factor receptor (TNFR superfamily, member 16)
1417122_at	0.0767	Vav3	Vav 3 oncogene; synonyms: AA986410, MGC27838, A530094I06Rik; isoform 2 is encoded by transcript variant 2; *Mus musculus* vav 3 oncogene (Vav3), transcript variant 2, mRNA.
1454254_s_at	0.072	Itgb1	Integrin beta 1 (fibronectin receptor beta)
1431711_a_at	0.07	Apbb2	Amyloid beta (A4) precursor protein-binding, family B, member 2
1429701_at	0.0689	2410003J06Rik	RIKEN cDNA 2410003J06 gene
1434739_at	0.0629	3830422N12Rik	RIKEN cDNA 3830422N12 gene
1429203_at	0.06	2410076I21Rik	RIKEN cDNA 2410076I21 gene
1423523_at	0.0587	Aass	Aminoadipate-semialdehyde synthase
1436799_at	0.0559	D230005D02Rik	RIKEN cDNA D230005D02 gene
1447021_at	0.0509		CDNA clone MGC:61032 IMAGE:30024827, complete cds
1419540_at	0.0496	Clec5a	C-type lectin domain family 5, member a
1420357_s_at	0.0474	Fndc6	Fibronectin type III domain containing 6
1448889_at	0.0334	Slc38a4	Solute carrier family 38, member 4
1419241_a_at	0.0192	Aire	Autoimmune regulator (autoimmune polyendocrinopathy candidiasis ectodermal dystrophy)
1453544_at	0.0184	4933424F23Rik	RIKEN cDNA 4933424F23 gene
1428111_at	0.0165	Slc38a4	Solute carrier family 38, member 4

[a] Average from three experiments.
[b] Some genes have multiple distinct probes on the GeneChip® resulting in different fold changes from different probes.

The number of genes expressed at higher levels in the F9 Wt cells relative to the F9 RARγ$^{-/-}$ cells was fivefold greater than the number of genes expressed at reduced levels (894 *versus* 164) in the control condition (vehicle-treated, 24 h) (Fig. 3). This could indicate that RARγ can mediate a substantial level of transcriptional activation in the absence of RA. A complete list of these genes is in the GEO database (www.ncbi.nlm.nih.gov/geo, accession # GSE8431).

3.4. *Distinctive expression profiles in the F9 Wt cell line following RA addition: RA-regulated genes*

RA-responsive genes in this F9 stem cell differentiation system were identified by comparing F9 Wt cells treated with 1 μM RA for 24 h *versus* F9 Wt cells treated with vehicle only (ethanol). Of the 45,037 gene transcripts, 345 gene transcripts (0.76%) exhibited at least a twofold difference in expression after RA treatment ($P \leq 0.05$, Welch's *t*-test). Among these, 190 (0.42%) of the gene transcripts are up-regulated and 155 (0.34%) of the gene transcripts are down-regulated by at least twofold after RA addition. The complete list of these 345 genes, including ESTs, can be found in the GEO database (www.ncbi.nlm.nih.gov/geo, accession # GSE8431).

Many known RA-responsive genes with RAREs were identified in this analysis. They include Cdx1, a number of Hox genes (Hox-a1, b1, a4), Cyp26A1, CRABPII, and RARβ (Appendix 1). The list also includes genes known to be RA-responsive, but which lack a well characterized RARE; they include AKP2, Stra6, CRABP1, Ptge1, CRBPII, (RBP2), KcNK6, Kitl, Lgals3, Lgals1, PDGFα, and Pik3r1 (P85α) [52]. We also found that some genes whose expression was known to be regulated by RA in other cell lines are also regulated by RA in F9 Wt cells. These genes include Gas1 [53], IL12b, Zfp503 [54], PMP22 [53,55], Nrip1 (Rip140) [56], C3 complement [57], keratin8, Gfra3, and Myosin light regulatory polypeptide 7.

We identified novel RA-regulated genes which exhibited greater than twofold changes compared to the levels of expression in untreated F9 Wt cells, such as Serum/glucocorticoid-regulated kinase 3, Topoisomerase (DNA) I, Musculin, plexin A2, Cullin 7, Akt2, serologically defined colon cancer antigen 33, Neuropilin 1, epididymal protein Av381126, Opioid receptor-like 1, Cathepsin B, Matrix metallopeptidase 15, ceroid-lipofuscinosis neuronal 8, vanin 1, endothelin receptor type B, Tuberous sclerosis 2, Chemokine (C-X-C motif) receptor 3, Eukaryotic translation initiation factor 5A2, growth factor receptor bound protein 2-associated protein 3, Microtubule-associated protein 4, and zinc finger protein 261 (Appendix 1).

3.5. *Expression profiles in the F9 Wt and RARγ$^{-/-}$ cell lines following RA addition: RA-regulated genes*

To identify RARγ-mediated, RA-responsive genes, we compared the differentially expressed genes between the two cell types to the RA-responsive genes in the F9 Wt cells in a Venn diagram (Fig. 4). Among the 345 probe sets which were identified as RA-responsive by at least a twofold change in expression levels after exposure to RA in F9 Wt cells, 161 probe sets were found to be differentially expressed between F9 Wt and RARγ$^{-/-}$ cells after a 24 h exposure to RA (Appendix 2).

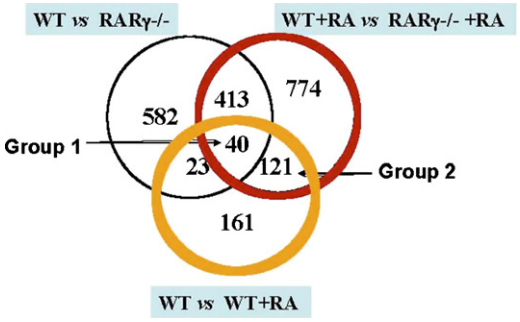

Fig. 4 – Venn diagram of 1058 genes (Wt *vs.* RARγ$^{-/-}$), 1348 genes (Wt + RA *vs.* RARγ$^{-/-}$ + RA) and 345 genes (Wt + RA *vs.* Wt). Genes from Fig. 3 were analyzed to determine which of the RA-responsive genes were also differentially expressed between the F9 Wt cells and F9 RARγ$^{-/-}$ cells.

Among the 1348 probe sets which were differentially expressed between the F9 Wt and RARγ$^{-/-}$ cell lines by at least twofold after 24 h-RA exposure, only a total of 161 probe sets were responsive to RA. These results indicate that 88% of these 1348 probe sets are not responsive to RA, or exhibit a less than twofold change after RA addition to F9 Wt cells. The changes in mRNA levels of these genes between the two cell types indicate that the majority of genes regulated by RARγ are not RA-regulated. However, some of the genes designated as RA non-responsive genes may be partially RA responsive. Their responsiveness to RA may be less than twofold, or the responsiveness to RA may occur at a later time point. Genes in this category include GATA4, GATA6, and laminin B1. Thus, the genes listed (Appendix 2) represent only the putative RARγ-mediated, RA-responsive genes at 24 h after RA addition.

3.6. *Real-time RT-PCR analyses of selected genes in F9 Wt, RARγ$^{-/-}$, RARα$^{-/-}$ and RARβ$_2^{-/-}$ cell lines in response to RA: Peg1/mest2, tie1, sfrp5, crygc, Zfp503, Runx-1 and Raet1a*

To validate the MG-430.2 microarray results and to determine if these RA-regulated genes are specifically regulated through RARγ, the mRNA levels of several of these genes were examined in the F9 Wt, RARγ$^{-/-}$, RARα$^{-/-}$, and RARβ$_2^{-/-}$ cell lines. The four cell lines were cultured in the presence or absence of RA for 6 h, 24 h, or 48 h. β-Actin mRNA was used for comparison. The mRNA levels of Peg1/mest2, sfrp5, crygc, Zfp503, Runx-1 and Raet1a were examined by real-time RT-PCR (Fig. 5). Tie1, a RARγ-regulated gene identified in our earlier gene chip (U74Av2) analyses, was also assessed by real-time quantitative RT-PCR (Fig. 5). These genes were selected for validation because they had relatively high fold changes and/or were found to have interesting biological functions.

Peg1/mest2 encodes "paternally expressed 1 (Peg1)/mesoderm-specific transcript (Mest)", and is an imprinted gene which is only transcribed from the paternal (father's) allele [58]. It is expressed predominantly in cells of the mesodermal lineage [59]. Our microarray data indicate that Peg1/mest mRNA levels are not regulated by RA in Wt F9 cells at 24 h (Appendix 2). Peg1/mest2 transcripts exhibit 18.6 ± 3.7-fold and 25.2 ± 6.9-fold higher levels in F9 Wt than in RARγ$^{-/-}$ cells in control and RA-treated samples, respectively. Peg1/mest

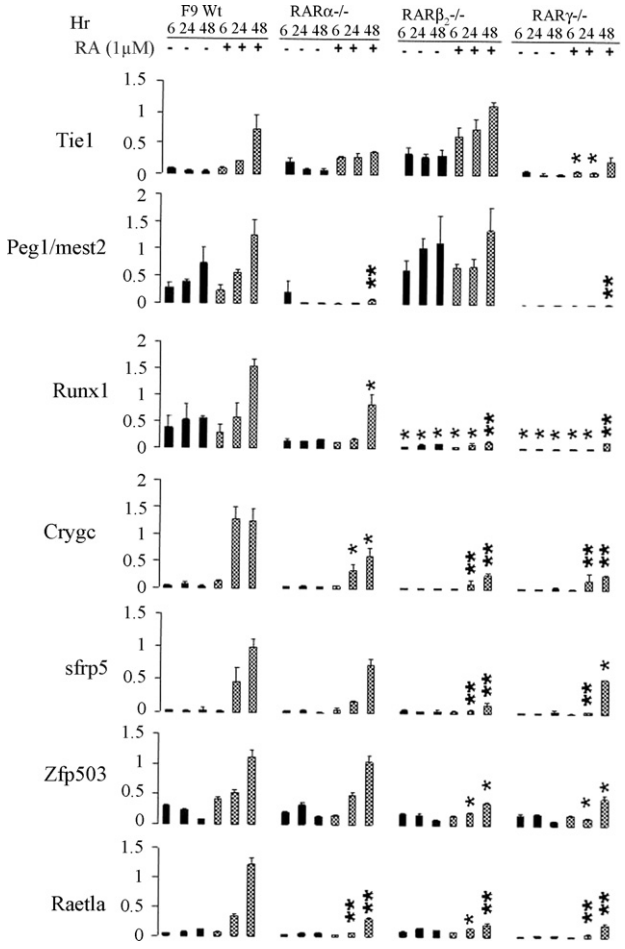

Fig. 5 – Real-time RT-PCR analyses of Tie1, Peg1/mest2, Runx-1, crygc, sfrp5, Zfp503, and Raet1a, in F9 Wt, RARγ$^{-/-}$, RARα$^{-/-}$, and RARβ$_2$$^{-/-}$ cell lines in response to RA. Total RNA was extracted from the F9 Wt, RAR γ$^{-/-}$, RARα$^{-/-}$, RARβ$_2$$^{-/-}$ cells cultured in the presence or absence of 1 μM RA for 6, 24, or 48 h. An equivalent amount of RNA (5 μg) was subjected to RT-PCR with primers specific for the indicated genes. Real-time quantitative (SYBR green) PCR of the indicated genes was performed and the mRNA levels were normalized to β-actin mRNA levels. The data are shown as fold increases in mRNA levels relative to the β-actin mRNA levels at each condition. Y axis, relative mRNA expression level. The results shown here are derived from three independent experiments with triplicates. The normalized mRNA levels of F9 RARα$^{-/-}$, RARβ$_2$$^{-/-}$, RARγ$^{-/-}$ cell samples were compared to F9 Wt cell samples at the respective time points and drug treatments for statistical significance. The unpaired Student's *t*-test was used to determine the *P* values. Bars, S.E.; *significant ($P < 0.05$), **very significant ($P < 0.001$) in comparisons of the RNA values in the mutants with those in F9 Wt treated under the same condition. (For interpretation of the references to color in this figure legend, the reader is referred to the web version of the article)

mRNA levels are lower in F9 RARα$^{-/-}$, RARβ$_2$$^{-/-}$, and RARγ$^{-/-}$ than in F9 Wt by 45.6-fold ($P < 0.001$), 0.37-fold ($P > 0.05$), and 50.2-fold ($P < 0.001$) at 6 h; 17.9-fold ($P < 0.001$), 0.8-fold ($P > 0.05$), and 77.8-fold ($P < 0.001$) at 24 h; 16.2-fold ($P < 0.001$), 0.92-fold ($P > 0.05$), and 91.9-fold ($P < 0.001$) at 48 h, respectively, by quantitative real-time RT-PCR (Fig. 5). Thus, Peg1/mest2 is a putative target gene of both RARγ and RARα.

Runx-1 belongs to the Runt-related (Runx) transcription factor family [60]. Runx1 regulates the differentiation of hematopoietic cells. Mutations in Runx1 are closely associated with human acute myeloid leukemia [61]. Runx1 is also involved in neuronal cell fate specification and the formation of axonal projections [62]. Our microarray data indicate that Runx1 mRNA levels were not responsive to RA in F9 Wt cells at 24 h, and were 11.3 ± 3.2-fold and 15.1 ± 4.5-fold higher in F9 Wt cells than in RARγ$^{-/-}$ cells in control and RA-treated samples, respectively. Runx-1 mRNA levels were increased by RA by 2.6 ± 0.6-fold in F9 Wt cells at 48 h (Fig. 4). A RA-associated increase in Runx1 mRNA levels of 4.2 ± 0.5-fold was also seen in RARα$^{-/-}$ cells at 48 h (Fig. 4). In addition, Runx-1 mRNA levels were 5–13-fold higher in F9 Wt than in RARγ$^{-/-}$ and RARβ$_2$$^{-/-}$ cells at all of the time points examined (Fig. 5). These results indicate that Runx-1 is a putative target gene of both RARγ and RARβ$_2$.

Crygc encodes gamma C-crystallin, a major component of the eye lens [63]. Mutations in the mouse *Crygs* gene were demonstrated to cause cataracts [64]. Our microarray data indicate that RA increased Crygc mRNA levels by 15.5 ± 2.2-fold in F9 Wt cells and that Crygc mRNA levels were 3.8 ± 0.9-fold higher in RA-treated F9 Wt cells than in RA-treated F9 RARγ$^{-/-}$ cells at 24 h. Real-time PCR assays confirmed that RA increased Crygc mRNA levels in F9 Wt cells by 16.9 ± 2.4-fold ($P < 0.001$) and 36.3 ± 2.1-fold ($P < 0.001$) at 24 h and 48 h, respectively (Fig. 5). Crygc mRNA levels were higher in F9 Wt than in F9 RARα$^{-/-}$, RARβ$^{-/-}$, and RARγ$^{-/-}$ cells by 3.8-fold ($P < 0.05$), 12.7-fold ($P < 0.001$), and 7.4-fold ($P < 0.001$) respectively, after a 24 h-RA treatment (Fig. 5).

Sfrp5 is a member of the *secreted frizzled-related protein* (*Sfrp*) gene family [41]. The secreted *Sfrp* proteins can bind Wnt molecules and inhibit Wnt signaling [41]. *Sfrp5* is expressed in the anterior visceral endoderm (AVE) and the ventral foregut endoderm of the early mouse embryo [65,66], though genetic evidence indicates that sfrp5 is not essential for axis development [67]. Abnormal down-regulation of Sfrp5 due to abnormal promoter methylation has been suggested in certain tumors [68–70]. The microarray data indicate that RA treatment increased Sfrp5 mRNA levels by 4.0 ± 1.2-fold in Wt F9 cells, and Sfrp5 mRNA levels were 24.6 ± 5.2-fold higher RA-treated F9 Wt than in RA-treated F9 RARγ$^{-/-}$ cells at 24 h. Real-time RT-PCR data confirmed that RA increased Sfrp5 mRNA levels by 3.2 ± 1.1-fold ($P < 0.05$) and 17.3 ± 2.4-fold ($P < 0.001$), at 24 h and 48 h, respectively, in F9 Wt cells (Fig. 5). Sfrp5 mRNA levels in F9 RARα$^{-/-}$, RARβ$_2$$^{-/-}$, and RARγ$^{-/-}$ cells were 2.6-fold ($P > 0.05$), 9.1-fold ($P < 0.001$), and 13.0-fold ($P < 0.001$) lower, respectively, than in F9 Wt cells after a 24 h-RA treatment (Fig. 5) and 1.3-fold ($P > 0.05$), 7.9-fold ($P < 0.05$), and 1.8-fold ($P < 0.05$) lower respectively, than F9 Wt cells after a 48 h-RA treatment (Fig. 5).

Zfp503 (also called *Nolz-1*) is a member of the nocA/elB/tlp-1 family [71]. Nolz-1 mRNA was dramatically induced upon neural induction of P19 embryonal carcinoma cells by RA [54].

Our microarray data indicate that RA increased Zfp503 mRNA levels by 21.9 ± 3.7-fold in F9 Wt cells, and Zfp503 mRNA levels were 5.2 ± 1.8-fold higher in RA-treated F9 Wt cells than in RA-treated F9 RARγ$^{-/-}$ cells at 24 h. RA increased Zfp503 mRNA levels by 2.2 ± 0.1-fold ($P < 0.05$) and 16.2 ± 2.9-fold ($P < 0.001$) at 24 h and 48 h, respectively, in F9 Wt cells as measured by real-time RT-PCR (Fig. 5). Zfp503 mRNA levels were 2.5-fold ($P < 0.05$) and 4.2-fold ($P < 0.001$) higher in F9 Wt than in F9 RARβ$_2^{-/-}$ and RARγ$^{-/-}$ cells, respectively, after a 24 h-RA treatment as measured by real-time RT-PCR (Fig. 5). These results indicate that Zfp503 is a putative target gene of both RARγ and RARβ$_2$.

Raet1a encodes a glycoprotein "retinoic acid early inducible protein 1 alpha precursor" (RAE-1alpha). The Rae proteins are anchored on the cell surface by a glycosyl phosphatidylinositol (GPI) tail [72], and act as ligands for a natural killer cell lectin-like receptor [73]. Rae proteins are not expressed in normal, healthy tissues in adult mice, but are induced by viral infection or cellular transformation, implying a role for Rae proteins in the regulation of immunity [74]. Our microarray data indicate that RA increased Raet1a mRNA levels by 6.4 ± 1.5-fold in F9 Wt cells, and Raet1a mRNA levels were 14.3 ± 2.6-fold higher in RA-treated F9 Wt cells than in RA-treated F9 RARγ$^{-/-}$ cells at 24 h. RA increased Raet1a mRNA levels in F9 Wt cells by 4.9 ± 1.1-fold ($P < 0.001$) and 11.1 ± 2.8-fold ($P < 0.001$) at 24 h and 48 h, respectively, by real-time RT-PCR (Fig. 5). After a 24 h-RA treatment, *Raet1a* mRNA levels were 6.2-fold ($P < 0.001$), 2.4-fold ($P < 0.05$), and 7.1-fold ($P < 0.001$) lower, respectively, in F9 RARα$^{-/-}$, RARβ$_2^{-/-}$, and RARγ$^{-/-}$ cells than in F9 Wt cells. These data indicate that all of these RARs are involved in the regulation of Raet1a.

Tie1 mRNA levels were 25.0 ± 8.2-fold higher in F9 Wt cells than in F9 RARγ$^{-/-}$ cells after a 24 h RA treatment (Table 2). Tie1 mRNA levels were also higher in F9 Wt cells than in F9 RARγ$^{-/-}$ cells as assessed by semi-quantitative RT-PCR (Fig. 2). Tie1 mRNA levels increased by 4.1 ± 0.1-fold ($P < 0.05$) and by 18.2 ± 3.1-fold ($P < 0.05$) at 24 h and 48 h after RA addition, respectively, in F9 Wt cells. Tie1 mRNA levels were 3.9-fold and 3.3-fold higher in F9 Wt cells than in F9 RARγ$^{-/-}$ cells at 24 h and 48 h after RA addition, respectively (Fig. 5). From these data (Fig. 5), the Tie1 gene has the characteristics of an RARγ-specific target gene.

3.7. Further analysis using DAVID

For the purpose of understanding how the loss of RARγ affects the biology of F9 cells, we chose to identify the biological processes associated with genes that show reduced or increased expression independently. DAVID identifies categories that are over-represented in the gene list relative to the representation within the genome of a given species. First, the functional annotation clustering tool displays similar annotations together in clusters. The grouping algorithm is based on the hypothesis that similar annotations should have similar gene members. The degree of common genes between two annotations is measured by *Kappa* statistics, and the *Kappa* values are then used to classify groups of similar annotations. Next, DAVID calculates the chances of over-representation of the clusters using the Fisher Exact test. The main benefit of over-representation analysis is to order categories associated with a gene list in order to focus on those processes most likely associated with the biological phenomenon under study; in this case, the biological phenomenon is the lack of RARγ function in F9 cells.

The major biological processes that were enriched in either F9 RARγ$^{-/-}$ cells or in F9 Wt cells, based on the differentially expressed genes, are shown (Table 5). Based on the genes that were expressed at higher levels in the control F9 RARγ$^{-/-}$ cells, the biological processes pattern specification, odontogenesis, and organic acid transport were the top terms to be enriched. Four organic acid transporter genes were expressed at higher mRNA levels in F9 RARγ$^{-/-}$ cells than in F9 Wt cells, including Slc43, Slc1a1, Slc38a4, and RIKEN cDNA 9130023d20. The control F9 RARγ$^{-/-}$ cells were highly enriched in genes involved in pattern specification, such as Otx2, Lef1, Fst, Mib1, and FGF4. The RA-treated F9 RARγ$^{-/-}$ cells were highly enriched in genes involved in ribosome biogenesis and cell migration, suggesting that RARγ activity plays a role in regulating ribosome biogenesis and cell migration in F9 cells. Five ribosome genes were expressed at higher mRNA levels in

Table 5 – Biological processes that are changed in F9 RARγ$^{-/-}$ cells as compared to F9 Wt cells at 24 h in the presence of RA or absence of RA, as indicated by DAVID analyses. "–", reduced processes; "+", increased processes

	Change in F9 RARγ$^{-/-}$ cells		
	Change	# of genes	P[a]
24 h-control			
Morphogenesis	–	73	4.4E−10
Lipid biosynthesis	–	22	2.7E−6
Zinc ion homeostasis	+	3	8.5E−4
Translational initiation	+	3	4.6E−2
A–P Pattern specification	+	4	4.5E−3
Odontogenesis	+	3	7.2E−3
24 h-RA			
Vasculature development	–	14	5.6E−3
Neurogenesis	–	17	1.4E−2
Ribosome biogenesis and assembly	+	13	7.0E−5
Cell migration	+	19	1.6E−3

[a] One-tail Fisher Exact probability value.

F9 RARγ$^{-/-}$ cells than in F9 Wt cells after a 24 h exposure to RA, including RpL36a, RpL27, mRpL22, RpS24, and RpS20. Genes involved in regulation of ribosome biogenesis including Ftsj3, Gtpb4, and Rrs1, were also expressed at higher mRNA levels in F9 RARγ$^{-/-}$ cells than in F9 Wt cells after a 24 h exposure to RA. The cell migration-related genes that had higher mRNA levels in F9 RARγ$^{-/-}$ cells than in F9 Wt cells include Pou4f2, Ngfr, Tdgf, Rtn4, jagged 2, enabled homolog, Ctgf, Tek, and PECAM-1.

The control F9 Wt cells were highly enriched in genes involved in cellular morphogenesis, such as *Smo*, *Gjb3*, and *Dkk1*, suggesting that RARγ activity is important for normal F9 cell morphogenesis. Genes up-regulated in 24 h-RA-treated F9 Wt cells were found to be enriched in the biological processes, cell differentiation, nervous system development, vasculature development, and angiogenesis categories, which indicates that F9 Wt cells are induced by RA to differentiate into certain cell lineages, and that these developmental programs require RARγ activity to proceed normally.

4. Discussion

4.1. Microarray analyses of F9 Wt versus F9 RARγ$^{-/-}$ cells

F9 teratocarcinoma stem cells normally undergo RA-induced differentiation by activating the transcription of genes involved in cellular differentiation and development, and repressing the transcription of stem cell genes [75]. However, how gene transcription on a genome-wide scale is affected when RARγ expression is abolished is poorly understand. The goal of this research was to identify genes which showed altered expression in the absence of RARγ in F9 cells. We chose to study mRNA levels at the genome-wide level by microarray analysis.

Despite the similarity of F9 Wt and F9 RARγ$^{-/-}$ cells in morphology and growth characteristics [76], the gene expression profiles in the two cell lines are distinctive. A total of 1058 probe sets were differentially expressed by greater than twofold between the F9 Wt and RARγ$^{-/-}$ cell lines in the *absence* of exogenously added RA, suggesting that RARγ controls gene transcription in the absence of its ligand. According to the current model of gene regulation by retinoids established by Dilworth and Chambon [77], unliganded and DNA-bound retinoid receptors repress transcription through the recruitment of the corepressors NCoR and SMRT [78]. However, transient transfection reporter assays have demonstrated that RARγ mediated substantial levels of transcriptional activation in the absence of RA, as did RARβ [79]. Our microarray data demonstrate that a far greater number of genes are expressed at a higher level rather than a lower level in the vehicle-treated, control F9 Wt cells relative to the vehicle-treated F9 RARγ$^{-/-}$ cells (Fig. 3). Our data are consistent with the idea that unliganded RARγ, a nuclear transcription factor, can activate gene transcription. Unliganded RARγ only weakly interacts with SMRT [79]. The intramolecular interactions between helix 3 and helix 12 of the ligand-binding domain of RARγ prevent corepressor binding [80]. Unliganded RARα, in contrast, has been shown to interact strongly with the nuclear corepressor SMRT, and RARα does repress transcription [79]. Recent studies indicate that the transcriptional activity of RARγ can also be modified by RARγ phosphorylation by ubiquitin-mediated proteasomal degradation of RARγ [81].

4.2. Comparison of this microarray research in F9 Wt cells with previous studies

There is a high similarity between the RA-responsive gene we identified in F9 Wt cells as compared to those identified by Eifert et al. [82], who used 0.5 μM of RA to treat F9 Wt cells for 24 h and used Affymetrix U74Av2 arrays for analysis. However, Eifert et al. detected a greater number of genes changed by twofold or more in expression by RA than we did, even though the murine U74Av2 arrays they used contained a lower number of probe sets. One reason is that the data selection criteria for the two experiments were different. We employed a filter first to select genes that gave a ''present'' call in at least 3 chips out of a total of 12 chips for further analysis. Thus, genes that were not expressed or were weakly expressed across more than nine microarray chips were not selected, even though their mRNA fold changes between RA-treated and vehicle-treated samples were large. An examination of the data analysis protocol described by Eifert et al. suggests that they did not apply such a filter in their analyses; all of the genes that were differentially expressed were subjected to fold change analyses. Second, different concentrations of RA were used in the two studies, which may affect subsets of genes that are sensitive to RA concentration. There is another report describing microarray analysis of F9 RARγ-mediated RA-responsive genes [76]. By comparison of our data with this study, there are some overlapping genes. However, because of the differences in the manner in which the microarray analyses were performed, the Parrella et al. report and our experimental design emphasized different aspects of the differentiation process. In our experiments we compared the differentially expressed genes between the F9 Wt and F9 RARγ$^{-/-}$ cells in the presence *versus* the absence of RA, while Parrella et al. [76] only compared differences in gene inducibility by RA between the two cell lines. These researchers also did not emphasize the quantitative differences in gene expression between the two cell lines. Quantitative differences in gene expression have important biological consequences, as demonstrated by the different developmental outcome resulting from a <2-fold variation in the expression of *Oct4* in mouse ES cells [83]. Thus, the comparison of quantitative differences in gene expression between F9 Wt and F9 RARγ$^{-/-}$ cells in the presence *versus* the absence of RA, coupled with bioinformatics analyses concerning gene functions, is much more helpful in understanding the phenotypic differences between the F9 Wt and RARγ$^{-/-}$ cell lines.

4.3. Complex molecular mechanisms of actions of RARs

Over the last 20 years, more than 532 genes have been put forward as either direct or indirect targets of RA in permissive cellular contexts (reviewed by Balmer and Blomhoff [92]). Our laboratory was the first to clone the Hoxa1 cDNA and show that it was a direct, primary RA target gene [84]. Transcriptional control of Hoxa1 by RA is driven by an RAR/RXR heterodimer bound to a DR_5 RARE [85,86]. Using chromatin

immunoprecipitation, Gillespie and Gudas showed that RA increased the RXRα's association with the Hoxa1 RARE [87,88]. In the past few years, additional genes were reported to be regulated by RARs through non-classical RAREs, via coordination of other transcription factors, or through indirect pathways which involved the actions of other transcription factors or through multiple phosphorylation sites of RAR [89–91]. As examined using TESS (Transcription Element Esearching Program, www.cbil.upenn.edu/tess), few of the RARγ-regulated genes identified in our microarray analyses contain classical RAREs in their 5′ or 3′ flanking regions. It is possible that RAREs are located further 5′ or 3′ of the genes, or that some of the genes are ''secondary'' target genes rather than ''primary'' targets of the RARs. Thus, more research is required to understand the detailed transcriptional mechanisms by which these genes are regulated by RARγ.

Acknowledgements

We thank members of the Gudas laboratory for scientific discussion. We thank Dr. Xiaohan Tang and Vasundhra Kashyap for reading and reviewing this manuscript and Karl Ecklund for editorial assistance. This research was supported by the National Cancer Institute (LJG) and in part by DOD predoctoral fellowship # W81XWH-04-1-0440 to DS.

Appendix A

RA responsive genes in the F9 Wt cells identified using MG-430.2

Affymetrix ID	Fold change[ab]	Gene symbol	Gene title
1449582_at	43.69	Cdx1	Caudal type homeo box 1
1427354_at	40.16	Hoxa4	Homeo box A4
1449397_at	35.68	Hoxb2	Homeo box B2
1418415_at	26.59	Il12b	Interleukin 12b
1455498_at	23.18		Transcribed sequence with weak similarity to protein pir:A43932 (*H. sapiens*) A43932 mucin 2 precursor, intestinal—human
1423836_at	21.98	Zfp503	Zinc finger protein 503
1422723_at	16.94	Stra6	Stimulated by retinoic acid gene 6
1422674_s_at	15.55	Crygb	Crystallin, gamma B
1453501_at	13.08	Il12b	Interleukin 12b
1422617_at	11.5	Top1	Topoisomerase (DNA) I
1435693_at	10.2	BC012256	cDNA sequence BC012256
1451191_at	9.91	Crabp1	Cellular retinoic acid binding protein I
1454906_at	8.227	Rarb	Retinoic acid receptor, beta
1419430_at	7.714	Cyp26a1	Cytochrome P450, family 26, subfamily a, polypeptide 1
1456229_at	7.222		H3122A02-3 NIA Mouse 15K cDNA Clone Set *Mus musculus* cDNA clone H3122A02 3′, mRNA sequence
1416855_at	7.03	Gas1	BB550400 RIKEN full-length enriched, 2 days pregnant adult female oviduct *Mus musculus* cDNA clone E230022A16 3′ similar to X65128 *M. musculus* gas1 mRNA, mRNA sequence
1420603_s_at	6.49	Sgk3	Serum/glucocorticoid regulated kinase 3
1418880_at	6.354	Gfra3	Glial cell line derived neurotrophic factor family receptor alpha 3
1448926_at	6.102	Hoxa5	Homeo box A5
1460379_at	6.055	Hoxb4	Homeo box B4
1420568_at	5.652	Msc	Musculin
1455037_at	5.247	Plxna2	Plexin A2
1422007_at	5.069	Krt8	Keratin 8
1420565_at	5.057	Hoxa1	Homeo box A1
1451481_s_at	5.049	Cul7	Cullin 7
1433428_x_at	4.912	Tgm2	Transglutaminase 2, C polypeptide
1436075_at	4.842	Sfrp5	Secreted frizzled-related sequence protein 5
1416149_at	4.695	Akt2	Thymoma viral proto-oncogene 2
1427233_at	4.662	Sdccag33	Serologically defined colon cancer antigen 33
1446358_at	4.603		0 day neonate cerebellum cDNA, RIKEN full-length enriched library, clone: C230033K16 product: unknown EST, full insert sequence
1418084_at	4.478	Nrp1	Neuropilin 1
1438512_at	4.414	LOC210321	Epididymal protein Av381126
1418445_at	4.405	Slc16a2	Solute carrier family 16 (monocarboxylic acid transporters), member 2
1423023_at	4.404	Sfrp5	Secreted frizzled-related sequence protein 5

Appendix A (*Continued*)

Affymetrix ID	Fold change[ab]	Gene symbol	Gene title
1421474_a_at	4.372	Capzb	Capping protein (actin filament) muscle Z-line, beta
1448494_at	4.321	Gas1	BB550400 RIKEN full-length enriched, 2 days pregnant adult female oviduct *Mus musculus* cDNA clone E230022A16 3′ similar to X65128 M. *musculus* gas1 mRNA, mRNA sequence
1449089_at	4.31	Nrip1	Synonyms: RIP140, 9630050P12, 6030458L20Rik; go_component: nucleus [goid 0005634] [evidence IDA] [pmid 9774688]; go_function: transcription co-repressor activity [goid 0003714] [evidence IDA] [pmid 9774688]; go_function: protein binding [goid 0005515] [evidence IPI] [pmid 9774688]; go_process: negative regulation of transcription from Pol II promoter [goid 0000122] [evidence IDA] [pmid 9774688]; *Mus musculus* nuclear receptor interacting protein 1 (Nrip1), mRNA.
1437277_x_at	4.262	Tgm2	Transglutaminase 2, C polypeptide
1434384_at	4.237	8430438I05Rik	Nuclear receptor interacting protein 1
1423835_at	4.207	Zfp503	Zinc finger protein 503
1418379_s_at	4.133	1700034M03Rik	RIKEN cDNA 1700034M03 gene
1418496_at	4.116	Foxa2	Forkhead box A2
1435261_at	4.087	4732416N19Rik	Adult male epididymis cDNA, RIKEN full-length enriched library, clone: 9230114I18 product: unknown EST, full insert sequence
1427433_s_at	4.024	5730446D14Rik	RIKEN cDNA 5730446D14 gene
1460605_at	4.02	AA606869	Similar to Homeobox protein goosecoid-like (GSC-2) (LOC381848), mRNA
1435184_at	4.013	B430320C24Rik	0 day neonate lung cDNA, RIKEN full-length enriched library, clone: E030020K21 product: weakly similar to HYPOTHETICAL 13.8 kDa PROTEIN [*Homo sapiens*], full insert sequence
1422099_a_at	3.99	Oprl1	Opioid receptor-like 1
1448327_at	3.961	AI747699	Expressed sequence AI747699
1417937_at	3.932	Ctsb	Cathepsin B
1439341_at	3.903		Transcribed sequences
1422008_a_at	3.886	Krt8	Keratin 8
1417133_at	3.777	Pmp22	Peripheral myelin protein
1439561_at	3.759	2010012O05Rik	BB322051 RIKEN full-length enriched, adult male adrenal gland *Mus musculus* cDNA clone B330007D01 3′, mRNA sequence
1420753_at	3.719	Kitl	Kit ligand
1419735_at	3.71	C3	Complement component 3
1449370_at	3.619	Sox4	SRY-box containing gene 4
1447211_at	3.611	Nrip1	Nuclear receptor interacting protein 1
1449071_at	3.572	Myl7	Myosin, light polypeptide 7, regulatory
1422597_at	3.572	Mmp15	Matrix metallopeptidase 15
1452303_at	3.485	Arhgef10	Ceroid-lipofuscinosis, neuronal 8
1426927_at	3.473	Ap3b2	Adaptor-related protein complex 3, beta 2 subunit
1418446_at	3.453	Slc16a2	Solute carrier family 16 (monocarboxylic acid transporters), member 2
1453286_at	3.445	Plxna2	BB085537 RIKEN full-length enriched, adult male diencephalon *Mus musculus* cDNA clone 9330200E06 3′, mRNA sequence
1440143_at	3.434	F630022B06Rik	RIKEN cDNA F630022B06 gene
1447845_s_at	3.404	Vnn1	Vanin 1
1454677_at	3.373	Timp2	Tissue inhibitor of metalloproteinase 2
1417500_a_at	3.367	Tgm2	Transglutaminase 2, C polypeptide
1418469_at	3.359	Nrip1	Synonyms: RIP140, 9630050P12, 6030458L20Rik; go_component: nucleus [goid 0005634] [evidence IDA] [pmid 9774688]; go_function: transcription co-repressor activity [goid 0003714] [evidence IDA] [pmid 9774688]; go_function: protein binding [goid 0005515] [evidence IPI] [pmid 9774688]; go_process: negative regulation of transcription from Pol II promoter [goid 0000122] [evidence IDA] [pmid 9774688]; *Mus musculus* nuclear receptor interacting protein 1 (Nrip1), mRNA.

Appendix A (*Continued*)

Affymetrix ID	Fold change[ab]	Gene symbol	Gene title
1433662_s_at	3.353	Timp2	Tissue inhibitor of metalloproteinase 2
1429134_at	3.347	2900056N03Rik	RIKEN cDNA 2900056N03 gene
1430425_at	3.328	5330435L01Rik	RIKEN cDNA 5330435L01 gene
1417956_at	3.325	Cidea	Cell death-inducing DNA fragmentation factor, alpha subunit-like effector A
1420150_at	3.316	4930422J18Rik	RIKEN cDNA 4930422J18 gene
1450460_at	3.233	Krt8	Keratin 8
1437347_at	3.217	Ednrb	Endothelin receptor type B
1448754_at	3.201	Rbp1	Retinol binding protein 1, cellular
1420831_at	3.19	Klhl22	Kelch-like 22 (*Drosophila*)
1456329_at	3.171	A230098A12Rik	RIKEN cDNA A230098A12 gene
1456481_at	3.169	D9Ertd280e	Hypothetical protein D930024E11
1418486_at	3.073	Edg2	Endothelial differentiation, lysophosphatidic acid G-protein-coupled receptor, 2
1449364_at	3.066	Aurkc	Aurora kinase C
1438682_at	3.054	Pik3r1	Hypothetical protein C530050K14 (C530050K14), mRNA
1432269_a_at	2.995	Sh3kbp1	SH3-domain kinase binding protein 1
1439747_at	2.987	Ptges	Prostaglandin E synthase
1460204_at	2.974	Tsc2	Tuberous sclerosis 2
1450624_at	2.955	Surf4	Surfeit gene 4
1419959_s_at	2.882	C330003B14Rik	RIKEN cDNA C330003B14 gene
1435743_at	2.882	C130068N17Rik	RIKEN cDNA C130068N17 gene
1449925_at	2.88	Cxcr3	Chemokine (C-X-C motif) receptor 3
1416674_at	2.862	Lyzs	Lysozyme
1438333_at	2.833	A230098A12Rik	RIKEN cDNA A230098A12 gene
1424194_at	2.82	Rcsd1	RCSD domain containing 1
1448000_at	2.804	Cdca3	AV352659 RIKEN full-length enriched, 11 days embryo gonad *Mus musculus* cDNA clone 7030413D12 3′, mRNA sequence
1429074_at	2.771	Eif5a2	Eukaryotic translation initiation factor 5A2
1428097_at	2.771	2510009E07Rik	RIKEN cDNA 2510009E07 gene, mRNA (cDNA clone IMAGE: 6491720), partial cds
1426589_at	2.722	Gab3	Growth factor receptor bound protein 2-associated protein 3
1460287_at	2.712	Timp2	Tissue inhibitor of metalloproteinase 2
1453622_s_at	2.699	Mllt3	Myeloid/lymphoid or mixed lineage-leukemia translocation to 3 homolog (*Drosophila*); synonyms: Af9, D4Ertd321e, 2210011H10Rik, 2610012I03Rik, 3830408D16Rik; isoform 2 is encoded by transcript variant 2; *Mus musculus* myeloid/lymphoid or mixed lineage-leukemia translocation to 3 homolog (*Drosophila*) (Mllt3), transcript variant 2, mRNA.
1424437_s_at	2.696	Mtap4	Microtubule-associated protein 4
1457829_at	2.681	Clgn	Calmegin
1430240_a_at	2.654	Clgn	Calmegin
1447326_s_at	2.638	Zfp261	Zinc finger protein 261
1415921_a_at	2.617	Tnf	Tumor necrosis factor
1419106_at	2.611	Tmem97	Transmembrane protein 97
1427195_at	2.61		Transcribed sequence with weak similarity to protein ref: NP_081764.1 (*M. musculus*) RIKEN cDNA 5730493B19 [*Mus musculus*]
1419155_a_at	2.597	Sox4	SRY-box containing gene 4
1429959_at	2.585	6620401D04Rik	12 days embryo female ovary cDNA, RIKEN full-length enriched library, clone: 6620401D04 product: interleukin 10 receptor, beta, full insert sequence
1439734_at	2.58		Transcribed sequence with weak similarity to protein pir:S12207 (*M. musculus*) S12207 hypothetical protein
1448470_at	2.578	Sod2	Superoxide dismutase 2, mitochondrial
1443882_at	2.575		Transcribed sequence with weak similarity to protein ref: NP_081764.1 (*M. musculus*) RIKEN cDNA 5730493B19 [*Mus musculus*]
1448825_at	2.568	Pdk2	Pyruvate dehydrogenase kinase, isoenzyme 2
1451277_at	2.551	Zfp131	Zinc finger protein 131

Appendix A (*Continued*)

Affymetrix ID	Fold change[ab]	Gene symbol	Gene title
1431602_a_at	2.547	1810064L21Rik	RIKEN cDNA A230065J02 gene
1455958_s_at	2.538	9130017A15Rik	RIKEN cDNA 9130017A15 gene
1420832_at	2.535	Klhl22	Kelch-like 22 (*Drosophila*)
1452141_a_at	2.534	Sepp1	Selenoprotein P, plasma, 1
1452302_at	2.534	Arhgef10	Ceroid-lipofuscinosis, neuronal 8
1449450_at	2.532	Ptges	Prostaglandin E synthase
1419602_at	2.524	Hoxa2	Homeo box A2
1458798_at	2.501		Transcribed sequences
1424334_at	2.497	Selpl	Selectin, platelet (p-selectin) ligand
1460337_at	2.454	Sh3kbp1	SH3-domain kinase binding protein 1
1455796_x_at	2.441	Olfm1	Olfactomedin 1
1448024_at	2.44	B430320C24Rik	0 day neonate lung cDNA, RIKEN full-length enriched library, clone: E030020K21 product: weakly similar to HYPOTHETICAL 13.8 kDa PROTEIN [*Homo sapiens*], full insert sequence
1417605_s_at	2.411	St3gal2	ST3 beta-galactoside alpha-2,3-sialyltransferase 2
1460206_at	2.406	Mybbp1a	MYB binding protein (P160) 1a
1450673_at	2.398	Col9a2	Procollagen, type IX, alpha 2
1429483_at	2.395	Ndp52l1	H3048G12-3 NIA Mouse 15K cDNA Clone Set *Mus musculus* cDNA clone H3048G12 3′, mRNA sequences
1435740_at	2.377	E330020C23	Hypothetical protein E330020C23
1454752_at	2.371	AI606861	Similar to dJ259A10.1 (ssDNA binding protein (SEB4D)) (LOC380843), mRNA
1448147_at	2.365	Tnf	Tumor necrosis factor
1433844_a_at	2.362	Dusp9	Dual specificity phosphatase 9
1439810_s_at	2.358	Pramel7	Preferentially expressed antigen in melanoma like 7
1420924_at	2.353	Timp2	Tissue inhibitor of metalloproteinase 2
1433795_at	2.352	Tgfbr3	18-day embryo whole body cDNA, RIKEN full-length enriched library, clone: 1110036H20 product: unknown EST, full insert sequence
1420774_a_at	2.343	4930570C03Rik	RIKEN cDNA 4930570C03 gene
1434856_at	2.342	A130096K20	Hypothetical protein A130096K20
1432331_a_at	2.338	Prrx2	Paired related homeobox 2
1418517_at	2.323	Gja4	Gap junction membrane channel protein alpha 4
1454877_at	2.315	Sertad4	16 days embryo head cDNA, RIKEN full-length enriched library, clone: C130018M11 product: unclassifiable, full insert sequence
1454727_at	2.296	AI173486	Expressed sequence AI173486
1425212_a_at	2.289	Tnf	Tumor necrosis factor
1417625_s_at	2.281	Cmkor1	Chemokine orphan receptor 1
1433575_at	2.281	Sox4	SRY-box containing gene 4
1448727_at	2.277	Bcl10	B-cell leukemia/lymphoma 10
1419276_at	2.255	Enpp1	Ectonucleotide pyrophosphatase/phosphodiesterase 1
1452861_at	2.245	2010300C02Rik	RIKEN cDNA 2010300C02 gene
1456210_at	2.241		Transcribed sequences
1433845_x_at	2.226	Dusp9	Dual specificity phosphatase 9
1430650_at	2.223	Zfp191	Zinc finger protein 191
1460570_at	2.217	2900019M05Rik	Piggy Bac transposable element derived 5
1447537_at	2.217	1500032P08Rik	Properdin factor, complement
1419301_at	2.216	Fzd4	602109129F1 NCI_CGAP_Kid14 *Mus musculus* cDNA clone IMAGE: 4237519 5′, mRNA sequence.
1419309_at	2.213	Pdpn	Podoplanin
1417794_at	2.197	Casp2	Caspase 2
1427401_at	2.185	Chrna5	Cholinergic receptor, nicotinic, alpha polypeptide 5
1458878_at	2.175	Yes	Yamaguchi sarcoma viral (v-yes) oncogene homolog
1434277_a_at	2.171	6430570G24	Adult male olfactory brain cDNA, RIKEN full-length enriched library, clone: 6430570G24 product: unknown EST, full insert sequence
1435342_at	2.17	Kcnk6	Potassium inwardly-rectifying channel, subfamily K, member 6
1450839_at	2.167	D0H4S114	DNA segment, human D4S114
1419157_at	2.159	Sox4	SRY-box containing gene 4
1434528_at	2.15	Aard	Alanine and arginine rich domain containing protein
1449110_at	2.146	App	Amyloid beta (A4) precursor protein
1454737_at	2.143	Dusp9	Dual specificity phosphatase 9

Appendix A (*Continued*)

Affymetrix ID	Fold change[ab]	Gene symbol	Gene title
1419693_at	2.143	Colec12	Collectin sub-family member 12
1450992_a_at	2.136	Meis1	Myeloid ecotropic viral integration site 1
1426514_at	2.133	Agrin	Agrin
1417604_at	2.13	St3gal2	ST3 beta-galactoside alpha-2,3-sialyltransferase 2
1418709_at	2.126	Adarb1	Adenosine deaminase, RNA-specific, B1
1426785_s_at	2.124	Mgll	Monoglyceride lipase
1449449_at	2.118	Ptges	Prostaglandin E synthase
1453836_a_at	2.112	Mgll	Monoglyceride lipase
1422088_at	2.102	Lmyc1	Lung carcinoma myc-related oncogene 1
1424951_at	2.089	Cacna1d	Calcium channel, voltage-dependent, L type, alpha 1D subunit
1454082_a_at	2.076	Giyd2	GIY-YIG domain containing 2
1419156_at	2.073	Sox4	SRY-box containing gene 4
1452888_at	2.061	1110034G24Rik	RIKEN cDNA 1110034G24 gene
1417129_a_at	2.059	Mrg1	Myeloid ecotropic viral integration site-related gene 1
1418617_x_at	2.05	Clgn	Calmegin
1426869_at	2.05	Boc	Biregional cell adhesion molecule-related/down-regulated by oncogenes (Cdon) binding protein
1460378_a_at	2.04	Myb; Tes	Myeloblastosis oncogene; synonyms: TESS, Tes1, Tes2, testin2, D6Ertd352e; isoform 2 is encoded by transcript variant 2; testin 2; *Mus musculus* testis derived transcript (Tes), transcript variant 2, mRNA
1418505_at	2.036	Ogdh	Oxoglutarate dehydrogenase (lipoamide)
1434069_at	2.035	BC067047	Adult male testis cDNA, RIKEN full-length enriched library, clone: 4930413J11 product: mitochondria located 1 homolog (human), full insert sequence
1442180_at	2.026	BC038059	cDNA sequence BC038059
1455642_a_at	2.023	Fbxo23	F-box only protein 23
1426991_at	2.016	1810048J11Rik	RIKEN cDNA 1810048J11 gene
1459818_x_at	2.014	Zfp261	Zinc finger protein 261
1434756_at	2.013	5430421B17	Frizzled homolog 4 (*Drosophila*)
1456475_s_at	2.01	Prkar2b	Protein kinase, camp-dependent regulatory, type II beta
1442308_at	2.006	Smyd4	SET and MYND domain containing 4
1418872_at	0.499	Arsk	Arylsulfatase K
1416967_at	0.499	Sox2	SRY-box containing gene 2
1458277_at	0.498	Ccl25	Chemokine (C–C motif) ligand 25
1424652_at	0.498	Kctd10	Potassium channel tetramerisation domain containing 10
1435436_at	0.497		Transcribed sequences
1443822_s_at	0.497	D10Ertd214e	DNA segment, Chr 10, ERATO Doi 214, expressed
1450728_at	0.496	Fjx1	AV230815 RIKEN full-length enriched, 0 day neonate skin *Mus musculus* cDNA clone 4632401J20 3′, mRNA sequence
1450282_at	0.496	Fgf4	Fibroblast growth factor 4
1421052_a_at	0.492	Sms	Spermine synthase
1430780_a_at	0.491	Pmm1	Phosphomannomutase 1
1428775_at	0.491	1110008L16Rik	RIKEN cDNA 1110008L16 gene
1416605_at	0.49	Prkcbp1	Protein kinase C binding protein 1
1416505_at	0.489	Nr4a1	Nuclear receptor subfamily 4, group A, member 1
1447703_x_at	0.489	3110024A21Rik	AV214133 RIKEN full-length enriched, ES cells *Mus musculus* cDNA clone 2410133J07 3′, mRNA sequence
1447934_at	0.488	9630033F20Rik	RIKEN cDNA 9630033F20 gene
1420964_at	0.488	Enc1	Ectodermal–neural cortex 1
1451026_at	0.487	Ftsj3	FtsJ homolog 3 (*E. coli*)
1459658_at	0.487	Mcm5	Minichromosome maintenance deficient 5, cell division cycle 46 (*S. cerevisiae*)
1428869_at	0.486	Nolc1	Nucleolar and coiled-body phosphoprotein 1
1421260_a_at	0.484	Pgk1	Phosphoglycerate kinase 1
1428069_at	0.483	Ubqln1	Ubiquilin 1
1444883_at	0.482	Tmem19	L0079C06-3 NIA Mouse E12.5 Female Mesonephros and Gonads cDNA Library *Mus musculus* cDNA clone L0079C06 3′, mRNA sequence
1430433_at	0.481	4933406J08Rik	RIKEN cDNA 4933406J08 gene
1450928_at	0.481	Idb4	Inhibitor of DNA binding 4

Appendix A (*Continued*)

Affymetrix ID	Fold change[ab]	Gene symbol	Gene title
1445924_at	0.48		Transcribed sequence with weak similarity to protein ref: NP_060730.1 (*H. sapiens*) hypothetical protein FLJ10891 [*Homo sapiens*]
1441243_at	0.478		Transcribed sequence with weak similarity to protein ref: NP_081764.1 (*M. musculus*) RIKEN cDNA 5730493B19 [*Mus musculus*]
1452609_at	0.477	1190005I06Rik	RIKEN cDNA 1190005I06 gene
1418649_at	0.477	Egln3	EGL nine homolog 3 (*C. elegans*)
1448272_at	0.477	Btg2	B-cell translocation gene 2, anti-proliferative
1444390_at	0.476		Transcribed sequences
1453251_at	0.476	Tyrp1	Tyrosinase-related protein 1
1435367_at	0.476	Mapk4	Mitogen-activated protein kinase 4
1417725_a_at	0.475	Mtvr2	Mammary tumor virus receptor 2
1430208_at	0.474	Pir	Pirin
1421113_at	0.474	Whrn	Whirlin
1448566_at	0.469	Cdc42	Cell division cycle 42 homolog (*S. cerevisiae*)
1415938_at	0.469	Spink3	Serine peptidase inhibitor, Kazal type 3
1422786_at	0.469	Slc30a1	Solute carrier family 30 (zinc transporter), member 1
1431193_at	0.464	2610524B04Rik	RIKEN cDNA 4932409F03 gene
1454197_a_at	0.464	Calb1	Calbindin-28K
1427640_a_at	0.463	Runx1t1	Runt-related transcription factor 1; translocated to, 1 (cyclin D-related)
1424880_at	0.463	Trib1	Tribbles homolog 1 (*Drosophila*)
1451123_at	0.462	D19Wsu12e	DNA segment, Chr 19, Wayne State University 12, expressed
1429937_at	0.461	AI662478; BB238373; 1700010I21Rik	RIKEN cDNA D530033C11 gene
1417780_at	0.459	Lass4	Longevity assurance homolog 4 (*S. cerevisiae*)
1428377_at	0.459	Btbd11	BTB (POZ) domain containing 11
1429123_at	0.457	Rab27a	RAB27A, member RAS oncogene family
1419700_a_at	0.455	Prom1	Prominin 1
1436865_at	0.454	F630021I08Rik	RIKEN cDNA F630021I08 gene
1433959_at	0.454	9630048M01Rik	RIKEN cDNA 9630048M01 gene
1456296_at	0.453	5832426L23Rik	RIKEN cDNA 5832426L23 gene
1455890_x_at	0.453	Snrpn	Small nuclear ribonucleoprotein N
1444292_at	0.453	D7Ertd143e	NACHT, LRR and PYD containing protein 12
1437554_at	0.452	Plec1	Plectin 1
1436319_at	0.452	Sulf1	Sulfatase 1
1423748_at	0.452	B830012B01; D530020C15Rik	Pyruvate dehydrogenase kinase, isoenzyme 1
1423259_at	0.451	Idb4	Inhibitor of DNA binding 4
1434815_a_at	0.45	AI874665	mq46b10.x1 Soares_thymus_2NbMT *Mus musculus* cDNA clone IMAGE:581755 3′, mRNA sequence
1419708_at	0.45	Wnt6	Wingless-related MMTV integration site 6
1427023_at	0.449	Phyhipl	RIKEN cDNA 4921522K17 gene
1449484_at	0.449	Hfe2	Hemochromatosis type 2 (juvenile) (human homolog)
1449187_at	0.448	Pdgfa	BB371842 RIKEN full-length enriched, 16 days embryo head *Mus musculus* cDNA clone C130061I20 3′, mRNA sequence
1447181_s_at	0.446	Slc7a7	Solute carrier family 7 (cationic amino acid transporter, y+ system), member 7
1424310_at	0.446	Mocs2	Molybdenum cofactor synthesis 2
1443435_at	0.445		Transcribed sequences
1423786_at	0.444	Eif2c3	Eukaryotic translation initiation factor 2C, 3
1424643_at	0.444	Tcof1	Treacher Collins Franceschetti syndrome 1, homolog
1428549_at	0.443	Ccdc3	Coiled-coil domain containing 3
1426041_a_at	0.442	Bre; Fgd4	Brain and reproductive organ-expressed protein; synonyms: Frabp, ZFYVE6, 9030023J02Rik, 9330209B17Rik; isoform beta is encoded by transcript variant beta; frabin; Fgd1-related F-actin-binding protein; *Mus musculus* FYVE, RhoGEF and PH domain containing 4 (Fgd4), transcript variant beta, mRNA.; isoform gamma is encoded by transcript variant gamma; *Mus musculus* FYVE, RhoGEF and PH domain containing 4 (Fgd4), transcript variant gamma, mRNA
1449996_a_at	0.441	Hspa8	Heat shock protein 8

Appendix A (*Continued*)

Affymetrix ID	Fold change[ab]	Gene symbol	Gene title
1449031_at	0.441	Cited1	Cbp/p300-interacting transactivator with Glu/Asp-rich carboxy-terminal domain 1
1420086_x_at	0.436	Fgf4	Fibroblast growth factor 4
1429442_at	0.433	4921503C21Rik	RIKEN cDNA 4921503C21 gene
1422887_a_at	0.432	Ctbp2	
1449146_at	0.431	Notch4	Notch gene homolog 4 (*Drosophila*)
1427537_at	0.428	EPIPL; EPIPL1;	Epiplakin 1
1443241_at	0.427	6230424I18Rik	13 days embryo stomach cDNA, RIKEN full-length enriched library, clone: D530023N15 product: unclassifiable, full insert sequence
1417392_a_at	0.426	My+lat1; AI790233	Solute carrier family 7 (cationic amino acid transporter, y+ system), member 7
1417061_at	0.426	Cdc42	Cell division cycle 42 homolog (*S. cerevisiae*)
1427364_a_at	0.423	Odc1	Ornithine decarboxylase, structural 1
1448931_at	0.421	F2rl1	Coagulation factor II (thrombin) receptor-like 1
1448568_a_at	0.418	Keap1	Kelch-like ECH-associated protein 1
1434705_at	0.417	D7Wsu87e	TRAF-binding protein
1451527_at	0.417	Pcolce2	Procollagen C-endopeptidase enhancer 2
1428283_at	0.412	Cyp2s1	Cytochrome P450, family 2, subfamily s, polypeptide 1
1434239_at	0.411	AA408556	Expressed sequence AA408556
1453072_at	0.411	Gpr160	G protein-coupled receptor 160
1452384_at	0.411	Enpp3	ectonucleotide pyrophosphatase/phosphodiesterase 3
1415944_at	0.411	Sdc1	Syndecan 1
1427302_at	0.409	Enpp3	Ectonucleotide pyrophosphatase/phosphodiesterase 3
1423747_a_at	0.409	B830012B01; D530020C15Rik	Pyruvate dehydrogenase kinase, isoenzyme 1
1418744_s_at	0.407	Musk	Muscle, skeletal, receptor tyrosine kinase
1448688_at	0.406	Podxl	Podocalyxin-like
1436227_at	0.4	Ebaf	Endometrial bleeding associated factor
1431425_a_at	0.399	4930535B03Rik	RIKEN cDNA 4930535B03 gene
1451502_at	0.394	Pla2g10	Phospholipase A2, group X
1444458_at	0.393		Transcribed sequence with moderate similarity to protein pir:S12207 (*M. musculus*) S12207 hypothetical protein
1422912_at	0.392	Bmp4	Bone morphogenetic protein 4
1433733_a_at	0.39	Cry1	Cryptochrome 1 (photolyase-like)
1434458_at	0.388	Fst	Follistatin
1438160_x_at	0.379	Slco4a1	AV348121 RIKEN full-length enriched, adult male olfactory bulb *Mus musculus* cDNA clone 6430631M08 3′, mRNA sequence
1449455_at	0.375	Ehd4	EH-domain containing 4
1442379_at	0.37		Transcribed sequences
1455692_x_at	0.37	1700097N02Rik	Adult male testis cDNA, RIKEN full-length enriched library, clone: 1700122G02 product: unknown EST, full insert sequence
1449109_at	0.365	Socs2	Suppressor of cytokine signaling 2
1420085_at	0.36	Fgf4	Fibroblast growth factor 4
1436562_at	0.359	Ddx58	RIKEN cDNA 6430573D20 gene
1416316_at	0.355	Slc27a2	Solute carrier family 27 (fatty acid transporter), member 2
1438861_at	0.349	Bnc2	RIKEN cDNA 5031434M05 gene
1449231_at	0.349	1110008L16Rik	RIKEN cDNA 1110008L16 gene
1432418_a_at	0.342	Ckmt1	Creatine kinase, mitochondrial 1, ubiquitous
1421385_a_at	0.339	Zfp191	Zinc finger protein 191
1424531_a_at	0.331	Tcea3	Transcription elongation factor A (SII), 3
1452004_at	0.325	Calca	Calcitonin/calcitonin-related polypeptide, alpha
1443786_at	0.321	Utf1	BB000218 RIKEN full-length enriched, ES cells XhoI/SstI *Mus musculus* cDNA clone 2410014O14 3′ similar to NM_009482 *Mus musculus* undifferentiated embryonic cell transcription factor 1 (Utf1), mRNA sequence
1438084_at	0.32		Transcribed sequences
1450771_at	0.319	Dgcr2	DiGeorge syndrome critical region gene 2
1417745_at	0.318	Hnrpu	Heterogeneous nuclear ribonucleoprotein U
1437004_at	0.318	C78977	Similar to tripartite motif-containing 43 (LOC236469), mRNA

Appendix A (*Continued*)

Affymetrix ID	Fold change[ab]	Gene symbol	Gene title
1416899_at	0.317	Utf1	Undifferentiated embryonic cell transcription factor 1
1426673_at	0.315	Cdh3	Cadherin 3
1425284_a_at	0.314	Ash; 2210402C08Rik; 2410003M20Rik; 4933437C11Rik	RAB27A, member RAS oncogene family
1422952_at	0.308	Ng23	
1440563_at	0.299		15 days embryo head cDNA, RIKEN full-length enriched library, clone: D930010N06 product: unknown EST, full insert sequence
1426431_at	0.294	Jag2	AV264681 RIKEN full-length enriched, adult male testis (DH10B) *Mus musculus* cDNA clone 4930502C11 3′ similar to Y14331 *Mus musculus* partial mRNA for jagged2 protein, clone MB16, mRNA sequence
1416630_at	0.289	Id3	Inhibitor of DNA binding 3
1432018_at	0.287	Mas1	MAS1 oncogene
1439260_a_at	0.286	Enpp3	BB039510 RIKEN full-length enriched, 13 days embryo male testis *Mus musculus* cDNA clone 6030443A19 3′, mRNA sequence.
1459469_at	0.28	C78516	Transcribed sequences
1437588_at	0.279	Pou4f2	POU domain, class 4, transcription factor 2
1426808_at	0.278	Lgals3	Lectin, galactose binding, soluble 3
1419930_at	0.271	D15Ertd55e	Transcribed sequences
1450194_a_at	0.27	c-myb; M16449; AI550390; MGC18531; Myb	Myeloblastosis oncogene; synonyms: c-myb, M16449, AI550390, MGC18531; isoform 2 is encoded by transcript variant 2; myb protein; tumor-specific myb protein; *Mus musculus* myeloblastosis oncogene (Myb), transcript variant 2, mRNA.
1438068_at	0.269		BB251859 RIKEN full-length enriched, 7 days neonate cerebellum *Mus musculus* cDNA clone A730048G08 3′, mRNA sequence
1450989_at	0.269	Tdgf1	Teratocarcinoma-derived growth factor
1425926_a_at	0.269	Otx2	Orthodenticle homolog 2 (*Drosophila*)
1423232_at	0.256	Map2k5	Mitogen activated protein kinase kinase 5
1440867_at	0.251	Spry4	Sprouty homolog 4 (*Drosophila*)
1439746_at	0.246	C130085G02Rik	RIKEN cDNA C130085G02 gene
1421317_x_at	0.245	c-myb; M16449; AI550390; MGC18531; Myb	Myeloblastosis oncogene; synonyms: c-myb, M16449, AI550390, MGC18531; isoform 2 is encoded by transcript variant 2; myb protein; tumor-specific myb protein; *Mus musculus* myeloblastosis oncogene (Myb), transcript variant 2, mRNA.
1422021_at	0.244	Spry4	Sprouty homolog 4 (*Drosophila*)
1438824_at	0.234	Slc20a1	Solute carrier family 20, member 1
1424942_a_at	0.219	Myc	Myelocytomatosis oncogene
1445669_at	0.217	Spry4	Sprouty homolog 4 (*Drosophila*)
1450177_at	0.217	Ngfr	Nerve growth factor receptor (TNFR superfamily, member 16)
1449064_at	0.212	Mab21l2	Mab-21-like 2 (*C. elegans*)
1430086_at	0.202	Chrna9	Cholinergic receptor, nicotinic, alpha polypeptide 9
1436657_at	0.202		LOC380738 (LOC380738), mRNA
1453345_at	0.196	3830408G10Rik	RIKEN cDNA 3830408G10 gene
1454974_at	0.151	Ntn1	Syntaxin 8
1423378_at	0.135	Adam23	A disintegrin and metalloprotease domain 23
1444823_at	0.131		Transcribed sequences
1420463_at	0.0989	Clnk	Cytokine-dependent hematopoietic cell linker
1457402_at	0.0939		0 day neonate lung cDNA, RIKEN full-length enriched library, clone: E030031B17 product: unknown EST, full insert sequence
1431711_a_at	0.0812	Apbb2	Amyloid beta (A4) precursor protein-binding, family B, member 2

F9 Wt cells were treated for 24 h with 1 μM RA or vehicle control. Only those genes with at least a twofold change in RA-treated F9 Wt cells relative to control-treated cells with P values ≤ 0.05 are shown. Fold change = F9 Wt + RA/F9 Wt control.

[a] Average from three experiments.

[b] Some genes have multiple distinct probes on the GeneChip® resulting in different fold changes from different probes.

Appendix B

RA-responsive genes with at least a twofold change in expression in F9 Wt cells relative to F9 RARγ$^{-/-}$ cells after RA treatment for 24 h

Affymetrix ID	Fold change[a,b]	Gene symbol	Gene title
1455498_at	122.6		Transcribed sequence with weak similarity to protein pir:A43932 (*H. sapiens*) A43932 mucin 2 precursor, intestinal—human
1423023_at	24.61	Sfrp5	Secreted frizzled-related sequence protein 5
1448926_at	22.68	Hoxa5	Homeo box A5
1437347_at	21.85	Ednrb	Endothelin receptor type B
1420603_s_at	14.36	Raet1a	Retinoic acid early transcript alpha
1433428_x_at	12.67	Tgm2	Transglutaminase 2, C polypeptide
1416855_at	12.61	Gas1	BB550400 RIKEN full-length enriched, 2 days pregnant adult female oviduct *Mus musculus* cDNA clone E230022A16 3′ similar to X65128 *M. musculus* gas1 mRNA, mRNA sequence
1450624_at	10.81	Bhmt	Betaine–homocysteine methyltransferase
1451191_at	9.949	Crabp2	Cellular retinoic acid binding protein II
1436075_at	8.714	Sfrp5	Secreted frizzled-related sequence protein 5
1437277_x_at	8.36	Tgm2	Transglutaminase 2, C polypeptide
1453501_at	8.34	Hoxb1	Homeo box B1
1448470_at	7.705	Fbp1	Fructose bisphosphatase 1
1421385_a_at	7.631	Myo7a	Myosin VIIa
1430425_at	6.958	5330435L01Rik	RIKEN cDNA 5330435L01 gene
1450839_at	6.684	D0H4S114	DNA segment, human D4S114
1420924_at	6.492	Timp2	Tissue inhibitor of metalloproteinase 2
1428097_at	6.483	2510009E07Rik	RIKEN cDNA 2510009E07 gene, mRNA (cDNA clone IMAGE:6491720), partial cds
1438512_at	6.477	LOC210321	Epididymal protein Av381126
1426785_s_at	6.38	Mgll	Monoglyceride lipase
1439810_s_at	6.263	Pramel7	Preferentially expressed antigen in melanoma like 7
1433662_s_at	5.664	Timp2	Tissue inhibitor of metalloproteinase 2
1427433_s_at	5.661	5730446D14Rik	RIKEN cDNA 5730446D14 gene
1454677_at	5.545	Timp2	Tissue inhibitor of metalloproteinase 2
1448494_at	5.482	Gas1	BB550400 RIKEN full-length enriched, 2 days pregnant adult female oviduct *Mus musculus* cDNA clone E230022A16 3′ similar to X65128 *M. musculus* gas1 mRNA, mRNA sequence
1417500_a_at	5.389	Tgm2	Transglutaminase 2, C polypeptide
1453836_a_at	5.373	Mgll	Monoglyceride lipase
1423835_at	5.279	Zfp503	Zinc finger protein 503
1451481_s_at	5.22	D630035O19Rik	RIKEN cDNA D630035O19 gene
1448825_at	5.09	Pdk2	Pyruvate dehydrogenase kinase, isoenzyme 2
1449397_at	5.047	Hoxb2	Homeo box B2
1450992_a_at	5.013	Meis1	Myeloid ecotropic viral integration site 1
1433795_at	4.994	Tgfbr3	18-day embryo whole body cDNA, RIKEN full-length enriched library, clone: 1110036H20 product: unknown EST, full insert sequence
1419430_at	4.84	Cyp26a1	Cytochrome P450, family 26, subfamily a, polypeptide 1
1447845_s_at	4.806	Vnn1	Vanin 1
1453286_at	4.747	Plxna2	BB085537 RIKEN full-length enriched, adult male diencephalon *Mus musculus* cDNA clone 9330200E06 3′, mRNA sequence
1438682_at	4.54	Pik3r1	Hypothetical protein C530050K14 (C530050K14), mRNA
1420831_at	4.52	Qscn6	Quiescin Q6
1419602_at	4.455	Hoxa2	Homeo box A2
1417937_at	4.35	Dact1	Dapper homolog 1, antagonist of beta-catenin (*Xenopus*)
1449449_at	4.129	Ptges	Prostaglandin E synthase
1448754_at	4.118	Rbp1	Retinol binding protein 1, cellular
1440143_at	4.067	F630022B06Rik	RIKEN cDNA F630022B06 gene
1418486_at	3.89	Vnn1	Vanin 1
1422674_s_at	3.854	Crygc	Crystallin, gamma C
1435342_at	3.836	Kcnk6	Potassium inwardly-rectifying channel, subfamily K, member 6
1451277_at	3.782	C530046K17Rik	RIKEN cDNA C530046K17 gene
1460287_at	3.777	Timp2	Tissue inhibitor of metalloproteinase 2
1422597_at	3.726	Mmp15	Matrix metalloproteinase 15
1420565_at	3.686	Hoxa1	Homeo box A1
1454906_at	3.557	Rarb	Retinoic acid receptor, beta
1415938_at	3.518	Spink3	Serine protease inhibitor, Kazal type 3
1419309_at	3.429	Gp38	Glycoprotein 38

Appendix B (*Continued*)

Affymetrix ID	Fold change[a,b]	Gene symbol	Gene title
1435184_at	3.393	B430320C24Rik	0 day neonate lung cDNA, RIKEN full-length enriched library, clone: E030020K21 product: weakly similar to HYPOTHETICAL 13.8 kDa PROTEIN [*Homo sapiens*], full insert sequence
1452302_at	3.393	Arhgef10	Ceroid-lipofuscinosis, neuronal 8
1422723_at	3.387	Stra6	Stimulated by retinoic acid gene 6
1420753_at	3.375	Tll	Tolloid-like
1420832_at	3.279	Qscn6	Quiescin Q6
1456481_at	3.272	D9Ertd280e	Hypothetical protein D930024E11
1419301_at	3.228	Fzd4	602109129F1 NCI_CGAP_Kid14 *Mus musculus* cDNA clone IMAGE: 4237519 5′, mRNA sequence
1418709_at	3.199	Cox7a1	Cytochrome c oxidase, subunit VIIa 1
1424194_at	3.175	BC025872	cDNA sequence BC025872
1434069_at	3.041	BC067047	Adult male testis cDNA, RIKEN full-length enriched library, clone: 4930413J11 product: mitochondria located 1 homolog (human), full insert sequence
1452303_at	2.966	Arhgef10	Ceroid-lipofuscinosis, neuronal 8
1424334_at	2.938	Fbxo23	F-box only protein 23
1449450_at	2.922	Ptges	Prostaglandin E synthase
1420774_a_at	2.863	4930583H14Rik	RIKEN cDNA 4930583H14 gene
1455642_a_at	2.809	Fbxo23	F-box only protein 23
1419693_at	2.805	Colec12	Collectin sub-family member 12
1434277_a_at	2.711	6430570G24	Adult male olfactory brain cDNA, RIKEN full-length enriched library, clone: 6430570G24 product: unknown EST, full insert sequence
1452141_a_at	2.71	Sepp1	Selenoprotein P, plasma, 1
1435693_at	2.62	BC012256	cDNA sequence BC012256
1448024_at	2.559	B430320C24Rik	0 day neonate lung cDNA, RIKEN full-length enriched library, clone: E030020K21 product: weakly similar to HYPOTHETICAL 13.8 kDa PROTEIN [*Homo sapiens*], full insert sequence
1419155_a_at	2.549	Sox4	SRY-box containing gene 4
1433575_at	2.506	Sox4	SRY-box containing gene 4
1460605_at	2.486	AA606869	Similar to Homeobox protein goosecoid-like (GSC-2) (LOC381848), mRNA
1418084_at	2.454	Nrp	Neuropilin
1419157_at	2.418	Sox4	SRY-box containing gene 4
1455796_x_at	2.418	Olfm1	Olfactomedin 1
1443882_at	2.393		Transcribed sequence with weak similarity to protein ref: NP_081764.1 (*M. musculus*) RIKEN cDNA 5730493B19 [*Mus musculus*]
1427195_at	2.36		Transcribed sequence with weak similarity to protein ref: NP_081764.1 (*M. musculus*) RIKEN cDNA 5730493B19 [*Mus musculus*]
1424951_at	2.347	1300006M19Rik	RIKEN cDNA 1300006M19 gene
1417133_at	2.329	Pmp22	Peripheral myelin protein
1448727_at	2.293	Tle6	Transducin-like enhancer of split 6, homolog of *Drosophila* E(spl)
1439341_at	2.261		Transcribed sequences
1435743_at	2.244	C130068N17Rik	RIKEN cDNA C130068N17 gene
1416674_at	2.235	Ptpru	Protein tyrosine phosphatase, receptor type, U
1418415_at	2.225	Hoxb5	Homeo box B5
1417605_s_at	2.209	Camk1	calcium/calmodulin-dependent protein kinase I
1456329_at	2.081	A230098A12Rik	RIKEN cDNA A230098A12 gene
1417956_at	2.055	Cidea	Cell death-inducing DNA fragmentation factor, alpha subunit-like effector A
1418445_at	2.006	Slc16a2	Solute carrier family 16 (monocarboxylic acid transporters), member 2
1457829_at	2.004	Clgn	Calmegin
1422912_at	0.497	Bmp4	Bone morphogenetic protein 4
1424643_at	0.483	Tcof1	Treacher Collins Franceschetti syndrome 1, homolog
1438824_at	0.466	Slc20a1	Solute carrier family 20, member 1
1460204_at	0.465	Tec	Cytoplasmic tyrosine kinase, Dscr28C related (*Drosophila*)
1444390_at	0.444		Transcribed sequences
1426041_a_at	0.426	Fgd4	FYVE, RhoGEF and PH domain containing 4
1435436_at	0.405		Transcribed sequences
1430433_at	0.405	4933406J08Rik	RIKEN cDNA 4933406J08 gene
1428283_at	0.401	Cyp2s1	Cytochrome P450, family 2, subfamily s, polypeptide 1
1424310_at	0.399	Mocs2	Molybdenum cofactor synthesis 2
1433733_a_at	0.396	Cry1	Cryptochrome 1 (photolyase-like)
1430780_a_at	0.394	Pmm1	Phosphomannomutase 1
1424942_a_at	0.391	Myc	Myelocytomatosis oncogene
1437588_at	0.391	Pou4f2	POU domain, class 4, transcription factor 2
1419735_at	0.39	Csnk	Casein kappa
1429937_at	0.379	D530033C11Rik	RIKEN cDNA D530033C11 gene
1416967_at	0.374	Sox2	SRY-box containing gene 2

Appendix B (Continued)

Affymetrix ID	Fold change[a,b]	Gene symbol	Gene title
1419930_at	0.372	D15Ertd55e	Transcribed sequences
1422887_a_at	0.364	Ctbp2	
1438861_at	0.357	Bnc2	RIKEN cDNA 5031434M05 gene
1431425_a_at	0.354	4930535B03Rik	RIKEN cDNA 4930535B03 gene
1451527_at	0.345	Pcolce2	procollagen C-endopeptidase enhancer 2
1454197_a_at	0.341	D19Ertd678e	Unnamed protein product; hypothetical protein (evidence: rsCDS, ProCrest, decoder, NCBI CDS Predictor, Longest-ORF) putative; *Mus musculus* adult male testis cDNA, RIKEN full-length enriched library, clone: 4933411H20 product: hypothetical protein, full insert sequence
1436865_at	0.335	F630021I08Rik	RIKEN cDNA F630021I08 gene
1449455_at	0.333	Hck	Hemopoietic cell kinase
1423259_at	0.332	Idb4	Inhibitor of DNA binding 4
1416899_at	0.329	Utf1	Undifferentiated embryonic cell transcription factor 1
1434705_at	0.329	D7Wsu87e	TRAF-binding protein
1416505_at	0.321	Nr4a1	Nuclear receptor subfamily 4, group A, member 1
1421317_x_at	0.314	Myb	Myeloblastosis oncogene
1443786_at	0.313	Utf1	BB000218 RIKEN full-length enriched, ES cells XhoI/SstI *Mus musculus* cDNA clone 2410014O14 3′ similar to NM_009482 *Mus musculus* undifferentiated embryonic cell transcription factor 1 (Utf1), mRNA sequence
1423748_at	0.312	D530020C15Rik	RIKEN cDNA D530020C15 gene
1428775_at	0.311	1110008L16Rik	RIKEN cDNA 1110008L16 gene
1449231_at	0.31	Zfp296	Zinc finger protein 296
1455692_x_at	0.308	1700097N02Rik	Adult male testis cDNA, RIKEN full-length enriched library, clone: 1700122G02 product: unknown EST, full insert sequence
1418649_at	0.302	Egln3	EGL nine homolog 3 (*C. elegans*)
1438160_x_at	0.301	Slco4a1	AV348121 RIKEN full-length enriched, adult male olfactory bulb *Mus musculus* cDNA clone 6430631M08 3′, mRNA sequence
1452609_at	0.298	1190005I06Rik	RIKEN cDNA 1190005I06 gene
1416605_at	0.292	Nola2	Nucleolar protein family A, member 2
1434239_at	0.288	AA408556	Expressed sequence AA408556
1442379_at	0.287		Transcribed sequences
1432018_at	0.281	Ascl2	Achaete-scute complex homolog-like 2 (*Drosophila*)
1420086_x_at	0.279	Fgf4	Fibroblast growth factor 4
1450282_at	0.277	Fgf4	Fibroblast growth factor 4
1449484_at	0.276	Stc2	Stanniocalcin 2
1416316_at	0.272	Slc27a2	Solute carrier family 27 (fatty acid transporter), member 2
1444292_at	0.27	D7Ertd143e	NACHT, LRR and PYD containing protein 12
1440563_at	0.269		15 days embryo head cDNA, RIKEN full-length enriched library, clone: D930010N06 product: unknown EST, full insert sequence
1451026_at	0.267	Ftsj3	FtsJ homolog 3 (*E. coli*)
1453345_at	0.26	3830408G10Rik	RIKEN cDNA 3830408G10 gene
1452004_at	0.259	Calca	Calcitonin/calcitonin-related polypeptide, alpha
1426431_at	0.252	Jag2	AV264681 RIKEN full-length enriched, adult male testis (DH10B) *Mus musculus* cDNA clone 4930502C11 3′ similar to Y14331 *Mus musculus* partial mRNA for jagged2 protein, clone MB16, mRNA sequence
1438084_at	0.221		Transcribed sequences
1418744_s_at	0.215	Tesc	Tescalcin
1417745_at	0.21	Cpn1	Carboxypeptidase N, polypeptide 1
1420085_at	0.208	Fgf4	Fibroblast growth factor 4
1453072_at	0.208	Gpr160	G protein-coupled receptor 160
1449146_at	0.199	Notch4	Notch gene homolog 4 (*Drosophila*)
1424531_a_at	0.191	Tcea3	Transcription elongation factor A (SII), 3
1436657_at	0.187		LOC380738 (LOC380738), mRNA
1452384_at	0.187	Enpp3	Ectonucleotide pyrophosphatase/phosphodiesterase 3
1426808_at	0.181	Lgals3	Lectin, galactose binding, soluble 3
1450989_at	0.18	Tdgf1	Teratocarcinoma-derived growth factor
1439746_at	0.126	C130085G02Rik	RIKEN cDNA C130085G02 gene
1423378_at	0.115	Adam23	A disintegrin and metalloprotease domain 23
1425926_a_at	0.0799	Otx2	Orthodenticle homolog 2 (*Drosophila*)
1450177_at	0.0773	Ngfr	Nerve growth factor receptor (TNFR superfamily, member 16)
1431711_a_at	0.07	9030409G11Rik	RIKEN cDNA 9030409G11 gene

Fold change = F9 Wt + RA/F9 RARγ$^{-/-}$ + RA.

[a] Average from three experiments.

[b] Some genes have multiple distinct probes on the GeneChip® resulting in different fold changes from different probes.

Appendix C

Primers used for RT-PCR

Common name	Sequence	Product size (bp)	GeneBank accession no.
Hoxa1 (sense) (antisense)	5′-TGG AGG AAG TGA GAA AGT TGG C-3′; 5′-ATG GGA GTC GAG AGG TTT CC-3′	485	NM_010449
FBP-2 (sense) (antisense)	5′-TCC TGT ATG AAT GCA ATC CTG T-3′; 5′-CAA TTG ACA AAG ACA AAG GGA AG-3′	232	D42083
Tie1 (sense) (antisense)	5′-CCT TTG CTC AGA TCG CAC TA-3′; 5′-ATG CTG CTT TAG GTG GAG GA-3′	381	X80764
EMP1 (sense) (antisense)	5′-CCT CTC CAT CAT CTT CTC CAT C-3′; 5′-GAC GTC AAG GAA GCA TCA GCA T-3′	620	X98471
EMP3 (sense) (antisense)	5′-CCT CTT CAT GTT CCA ACT CTA-3′; 5′-TTT CCG CAG GTG GAT GTA GAC-3′	238	NM_010129
Sfrp2 (sense) (antisense)	5′-CAA CCT GCT GGG CCA CGA GAC C-3′; 5′-GCT TGC GGA TGC TGC GGG AGA T-3′	695	NM_009144
Sfrp5 (sense) (antisense)	5′-CTA TCC CTG TTC CCT CTA CTA C-3′; 5′-AGA ACC CTT CAG TCA AAG AGG G-3′	240	NM_018780
Coch5B2 (sense) (antisense)	5′-GGG CAG TCC TAT GAT GAT GT-3′; 5′-CCT TGCACG TAT TCC TTG AG-3′	243	AF006741
mOTT3 (sense) (antisense)	5′-ATC TCA TCA TGA CCA CTC AGG G-3′; 5′-TTC TTC GAT GTT CCT GTA CCC A-3′	267	NM_011022
Slc27a2 (sense) (antisense)	5′-AGT TCT ACG CAT CCA CTG AAG-3′; 5′-TGA CTG TGG GAT TGA AGC CCT CTT-3′	655	AF072757
Xlr3b (sense) (antisense)	5′-AGG CTG CCT TGT GGA GAG-3′; 5′-CTG TTG CCT CTC TGT TCC TG-3′	231	NM_011727
Runx-1 (sense) (antisense)	5′-CCA GCA AGC TGA GGA GCG GCG-3′; 5′-CGG ATT TGT AAA GAC GGT GA-3′	348	NM_009821
Crygc (sense) (antisense)	5′-CTG ACT ACC AGC AGT GGA TGG G-3′; 5′-CCT CAC TGA GGT GGA AGC GAT C-3′	171	NM_007775
Zfp503 (sense) (antisense)	5′-GCC TTT TGT GCA CGC TGT-3′; 5′-ACCGAG AGT TTG GAA GA-3′	243	AK032903
Raet1a (sense) (antisense)	5′-GCC ACT CTA CTT CTA AGA AAG GAT T-3′; 5′-GTG AAG CTT ACT GTG GGA CTT-3′	307	NM_009016
Peg1/Mest(sense) (antisense)	5′-ATT CGC AAC AAT GAC GGC-3′; 5′-TGA GGT GGA CTA TTG TGT CAC C-3′	441	BC006639
RARα (sense) (antisense)	5′-ATC GAG ACC CAG AGC AGC AG-3′; 5′-CCT GGT GCG CTT TGC GAA CC-3′	409	NM_009024
RARβ (sense) (antisense)	5′-GCA GAG TTT GAT GGA GTT CGT-3′; 5′-CCC ACT TCA AAG CAC TTC TGC A-3′	507	NM_011243
RARγ (sense) (antisense)	5′-CAA TAA GGA GAG ACT CTT TGC G-3′; 5′-TAC CAC TAT GGG GTC AGC TCC TGT G-3′	324	NM_011244
Neo-RARγ (sense) (antisense)	5′-ATT CGC AGC GCA TCG CCT TCT AT-3′; 5′-TTG CTG ACC TTG GTG ATG AGT-3′	612	NM_011244
Actin (sense) (antisense)	5′-AAG TGT GAC GTT GAC ATC CG-3′; 5′-GAT CCA CAT CTG CTG GAA GG-3′	222	NM_007393

REFERENCES

[1] Hayden LJ, Hawk SN, Sih TR, Satre MA. Metabolic conversion of retinol to retinoic acid mediates the biological responsiveness of human mammary epithelial cells to retinol. J Cell Physiol 2001;186:437–47.

[2] Napoli JL. A gene knockout corroborates the integral function of cellular retinol-binding protein in retinoid metabolism. Nutr Rev 2000;58:230–6.

[3] Blomhoff R, Blomhoff HK. Overview of retinoid metabolism and function. J Neurobiol 2006;66(7):606–30.

[4] Love JM, Gudas LJ. Vitamin A, differentiation and cancer. Curr Opin Cell Biol 1994;6:825–31.

[5] Altucci L, Rossin A, Raffelsberger W, Reitmair A, Chomienne C, Gronemeyer H. Retinoic acid-induced apoptosis in leukemia cells is mediated by paracrine action of tumor-selective death ligand TRAIL. Nat Med 2001;7(6):680–6.

[6] Chambon P. A decade of molecular biology of retinoic acid receptors. FASEB J 1996;10:940–54.

[7] Kastner P, Mark M, Chambon P. Nonsteroid nuclear receptors: what are genetic studies telling us about their role in real life? Cell 1995;83:859–69.

[8] Mangelsdorf DJ, Thummel C, Beato M, Herrlich P, Schütz G, Umesono K, et al. The nuclear receptor superfamily: the second decade. Cell 1995;83:835–40.

[9] Gudas LJ. Retinoids and vertebrate development. J Biol Chem 1994;269:15399–402.

[10] Means AL, Gudas LJ. The roles of retinoids in vertebrate development. Annu Rev Biochem 1995;64:201–33.

[11] Taneja R, Bouillet P, Boylan JF, Gaub MP, Roy B, Gudas LJ, et al. Reexpression of retinoic acid receptor

(RAR)γ or RARβ in RARγ-null F9 cells reveals a partial functional redundancy between the three RAR types. Proc Natl Acad Sci 1995;92:7854–8.
[12] Mark M, Ghyselinck NB, Chambon P. Function of retinoid nuclear receptors: lessons from genetic and pharmacological dissections of the retinoic acid signaling pathway during mouse embryogenesis. Annu Rev Pharmacol Toxicol 2006;46:451–80.
[13] Allan D, Houle M, Bouchard N, Meyer BI, Gruss P, Lohnes D. RARgamma and Cdx1 interactions in vertebral patterning. Dev Biol 2001;240(1):46–60.
[14] Wendling O, Ghyselinck NB, Chambon P, Mark M. Roles of retinoic acid receptors in early embryonic morphogenesis and hindbrain patterning. Development 2001;128:2031–8.
[15] Ghyselinck NB, Chapellier B, Calleja C, Kumar Indra A, Li M, Messaddeq N, et al. Genetic dissection of retinoic acid function in epidermis physiology. Ann Dermatol Venereol 2002;129(5 Pt 2):793–9.
[16] Chapellier B, Mark M, Messaddeq N, Calleja C, Warot X, Brocard J, et al. Physiological and retinoid-induced proliferations of epidermis basal keratinocytes are differently controlled. EMBO J 2002;21(13):3402–13.
[17] Iulianella A, Lohnes D. Chimeric analysis of retinoic acid receptor function during cardiac looping. Dev Biol 2002;247(1):62–75.
[18] McGowan S, Jackson SK, Jenkins-Moore M, Dai HH, Chambon P, Snyder JM. Mice bearing deletions of retinoic acid receptors demonstrate reduced lung elastin and alveolar numbers. Am J Respir Cell Mol Biol 2000;23(2):162–7.
[19] Purton LE, Dworkin S, Olsen GH, Walkley CR, Fabb SA, Collins SJ, et al. RARgamma is critical for maintaining a balance between hematopoietic stem cell self-renewal and differentiation. J Exp Med 2006;203(5):1283–93.
[20] Dzhagalov I, Chambon P, He YW. Regulation of CD8+ T lymphocyte effector function and macrophage inflammatory cytokine production by retinoic acid receptor gamma. J Immunol 2007;178(4):2113–21.
[21] Spanjaard RA, Ikeda M, Lee PJ, Charpentier B, Chin WW, Eberlein TJ. Specific activation of retinoic acid receptors (RARs) and retinoid X receptors reveals a unique role for RARgamma in induction of differentiation and apoptosis of S91 melanoma cells. J Biol Chem 1997;272(30):18990–9.
[22] Meister B, Fink FM, Hittmair A, Marth C, Widschwendter M. Antiproliferative activity and apoptosis induced by retinoic acid receptor-gamma selectively binding retinoids in neuroblastoma. Anticancer Res 1998;18(3A):1777–86.
[23] Hatoum A, El-Sabban ME, Khoury J, Yuspa SH, Darwiche N. Overexpression of retinoic acid receptors alpha and gamma into neoplastic epidermal cells causes retinoic acid-induced growth arrest and apoptosis. Carcinogenesis 2001;22(12):1955–63.
[24] Pettersson F, Dalgleish AG, Bissonnette RP, Colston KW. Retinoids cause apoptosis in pancreatic cancer cells via activation of RAR-gamma and altered expression of Bcl-2/Bax. Br J Cancer 2002;87(5):555–61.
[25] Siegrist W, Hintermann E, Roggo CN, Apfel CM, Klaus M, Eberle AN. Melanoma cell growth inhibition and melanocortin receptor downregulation induced by selective and non-selective retinoids. Melanoma Res 1998;8(2):113–22.
[26] Strickland S, Smith KK, Marotti KR. Hormonal induction of differentiation in teratocarcinoma stem cells: generation of parietal endoderm by retinoic acid and dibutyryl cAMP. Cell 1980;21(2):347–55.
[27] Wang S-Y, Gudas LJ. Isolation of cDNA clones specific for collagen IV and laminin from mouse teratocarcinoma cells. Proc Natl Acad Sci 1983;80:5880–4.
[28] Wang SY, LaRosa GJ, Gudas LJ. Molecular cloning of gene sequences transcriptionally regulated by retinoic acid and dibutyryl cyclic AMP in cultured mouse teratocarcinoma cells. Dev Biol 1985;107(1):75–86.
[29] Hogan BLM, Barlow D, Tilly R. F9 teratocarcinoma cells as a model for the differentiation of parietal and visceral endoderm in the mouse. Cancer Surv 1983;2:115–40.
[30] Boylan JF, Lohnes D, Taneja R, Chambon P, Gudas LJ. Loss of retinoic acid receptor gamma function in F9 cells by gene disruption results in aberrant Hoxa-1 expression and differentiation upon retinoic acid treatment. Proc Natl Acad Sci USA 1993;90(20):9601–5.
[31] Faria TN, Mendelsohn C, Chambon P, Gudas LJ. The targeted disruption of both alleles of RARbeta(2) in F9 cells results in the loss of retinoic acid-associated growth arrest. J Biol Chem 1999;274(38):26783–8.
[32] Boylan JF, Lufkin T, Achkar CC, Taneja R, Chambon P, Gudas LJ. Targeted disruption of retinoic acid receptor alpha (RAR alpha) and RAR gamma results in receptor-specific alterations in retinoic acid-mediated differentiation and retinoic acid metabolism. Mol Cell Biol 1995;15(2):843–51.
[33] Zhuang Y, Faria TN, Chambon P, Gudas LJ. Identification and characterization of retinoic acid receptor beta2 target genes in F9 teratocarcinoma cells. Mol Cancer Res 2003;1(8):619–30.
[34] Boylan JF, Lufkin T, Achkar CC, Taneja R, Chambon P, Gudas LJ. Targeted disruption of retinoic acid receptor α (RAR α) and RAR γ results in receptor-specific alterations in retinoic acid-mediated differentiation and retinoic acid metabolism. Mol Cell Biol 1995;15:843–51.
[35] Abu-Abed SS, Beckett BR, Chiba H, Chithalen JV, Jones G, Metzger D, et al. Mouse P450RAI (CYP26) expression and retinoic acid-inducible retinoic acid metabolism in F9 cells are regulated by retinoic acid receptor gamma and retinoid X receptor alpha. J Biol Chem 1998;273(4):2409–15.
[36] Wu C, Khan SA, Peng LJ, Lange AJ. Roles for fructose-2, 6-bisphosphate in the control of fuel metabolism: beyond its allosteric effects on glycolytic and gluconeogenic enzymes. Adv Enzyme Regul 2006;46:72–88.
[37] Korhonen J, Lahtinen I, Halmekyto M, Alhonen L, Janne J, Dumont D, et al. Endothelial-specific gene expression directed by the tie gene promoter in vivo. Blood 1995;86(5):1828–35.
[38] Puri MC, Rossant J, Alitalo K, Bernstein A, Partanen J. The receptor tyrosine kinase TIE is required for integrity and survival of vascular endothelial cells. EMBO J 1995;14(23):5884–91.
[39] Eklund L, Olsen BR. Tie receptors and their angiopoietin ligands are context-dependent regulators of vascular remodeling. Exp Cell Res 2006;312(5):630–41.
[40] Liehr T, Kuhlenbaumer G, Wulf P, Taylor V, Suter U, Van Broeckhoven C, et al. Regional localization of the human epithelial membrane protein genes 1.2, and 3 (EMP1, EMP2, EMP3) to 12p12. 3, 16p13. 2, and 19q13. 3. Genomics 1999;58(1):106–8.
[41] Jones SE, Jomary C. Secreted frizzled-related proteins: searching for relationships and patterns. Bioessays 2002;24(9):811–20.
[42] Boulassel MR, Tomasi JP, Deggouj N, Gersdorff M. COCH5B2 is a target antigen of anti-inner ear antibodies in autoimmune inner ear diseases. Otol Neurotol 2001;22(5):614–8.
[43] Robertson NG, Skvorak AB, Yin Y, Weremowicz S, Johnson KR, Kovatch KA, et al. Mapping and characterization of a novel cochlear gene in human and in mouse: a positional candidate gene for a deafness disorder, DFNA9. Genomics 1997;46(3):345–54.

[44] Robertson NG, Lu L, Heller S, Merchant SN, Eavey RD, McKenna M, et al. Mutations in a novel cochlear gene cause DFNA9, a human nonsyndromic deafness with vestibular dysfunction. Nat Genet 1998;20(3):299–303.
[45] Eavey RD, Manolis EN, Lubianca J, Merchant S, Seidman JG, Seidman C. Mutations in COCH (formerly Coch5b2) cause DFNA9. Adv Otorhinolaryngol 2000;56:101–2.
[46] Wang PJ, McCarrey JR, Yang F, Page DC. An abundance of X-linked genes expressed in spermatogonia. Nat Genet 2001;27(4):422–6.
[47] Hiriart E, Gruffat H, Buisson M, Mikaelian I, Keppler S, Meresse P, et al. Interaction of the Epstein-Barr virus mRNA export factor EB2 with human Spen proteins SHARP, OTT1, and a novel member of the family, OTT3, links Spen proteins with splicing regulation and mRNA export. J Biol Chem 2005;280(44):36935–4.
[48] Hirsch D, Stahl A, Lodish HF. A family of fatty acid transporters conserved from mycobacterium to man. Proc Natl Acad Sci USA 1998;95(15):8625–9.
[49] Raefski AS, O'Neill MJ. Identification of a cluster of X-linked imprinted genes in mice. Nat Genet 2005;37(6):620–4.
[50] Davies W, Isles A, Smith R, Karunadasa D, Burrmann D, Humby T, et al. Xlr3b is a new imprinted candidate for X-linked parent-of-origin effects on cognitive function in mice. Nat Genet 2005;37(6):625–9.
[51] Banerjee A, Xu HJ, Hu SX, Araujo D, Takahashi R, Stanbridge EJ, et al. Changes in growth and tumorigenicity following reconstitution of retinoblastoma gene function in various human cancer cell types by microcell transfer of chromosome 13. Cancer Res 1992;52(22):6297–304.
[52] Bastien J, Plassat JL, Payrastre B, Rochette-Egly C. The phosphoinositide 3-kinase/Akt pathway is essential for the retinoic acid-induced differentiation of F9 cells. Oncogene 2006;25(14):2040–7.
[53] Wang L, Mear JP, Kuan CY, Colbert MC. Retinoic acid induces CDK inhibitors and growth arrest specific (Gas) genes in neural crest cells. Dev Growth Differ 2005;47(3):119–30.
[54] Chang CW, Tsai CW, Wang HF, Tsai HC, Chen HY, Tsai TF, et al. Identification of a developmentally regulated striatum-enriched zinc-finger gene, Nolz-1, in the mammalian brain. Proc Natl Acad Sci USA 2004;101(8):2613–8.
[55] Wulf P, Suter U. Embryonic expression of epithelial membrane protein 1 in early neurons. Brain Res Dev Brain Res 1999;116(2):169–80.
[56] Kerley JS, Olsen SL, Freemantle SJ, Spinella MJ. Transcriptional activation of the nuclear receptor corepressor RIP140 by retinoic acid: a potential negative-feedback regulatory mechanism. Biochem Biophys Res Commun 2001;285(4):969–75.
[57] Scantlebury T, Sniderman AD, Cianflone K. Regulation by retinoic acid of acylation-stimulating protein and complement C3 in human adipocytes. Biochem J 2001;356(Pt 2):445–52.
[58] Kaneko-Ishino T, Kuroiwa Y, Miyoshi N, Kohda T, Suzuki R, Yokoyama M, et al. Peg1/Mest imprinted gene on chromosome 6 identified by cDNA subtraction hybridization. Nat Genet 1995;11(1):52–9.
[59] Reule M, Krause R, Hemberger M, Fundele R. Analysis of Peg1/Mest imprinting in the mouse. Dev Genes Evol 1998;208(3):161–3.
[60] Ito Y. Oncogenic potential of the RUNX gene family: 'overview'. Oncogene 2004;23(24):4198–208.
[61] de Bruijn MF, Speck NA. Core-binding factors in hematopoiesis and immune function. Oncogene 2004;23(24):4238–48.
[62] Yoshikawa M, Senzaki K, Yokomizo T, Takahashi S, Ozaki S, Shiga T. Runx1 selectively regulates cell fate specification and axonal projections of dorsal root ganglion neurons. Dev Biol 2007;303(2):663–74.
[63] Graw J. The crystallins: genes, proteins and diseases. Biol Chem 1997;378(11):1331–48.
[64] Graw J, Neuhauser-Klaus A, Klopp N, Selby PB, Loster J, Favor J. Genetic and allelic heterogeneity of Cryg mutations in eight distinct forms of dominant cataract in the mouse. Invest Ophthalmol Vis Sci 2004;45(4):1202–13.
[65] Finley KR, Tennessen J, Shawlot W. The mouse secreted frizzled-related protein 5 gene is expressed in the anterior visceral endoderm and foregut endoderm during early post-implantation development. Gene Expr Patterns 2003;3(5):681–4.
[66] Kemp C, Willems E, Abdo S, Lambiv L, Leyns L. Expression of all Wnt genes and their secreted antagonists during mouse blastocyst and postimplantation development. Dev Dyn 2005;233(3):1064–75.
[67] Leaf I, Tennessen J, Mukhopadhyay M, Westphal H, Shawlot W. Sfrp5 is not essential for axis formation in the mouse. Genesis 2006;44(12):573–8.
[68] Roman-Gomez J, Cordeu L, Agirre X, Jimenez-Velasco A, San Jose-Eneriz E, Garate L, et al. Epigenetic regulation of Wnt-signaling pathway in acute lymphoblastic leukemia. Blood 2007;109(8):3462–9.
[69] Nojima M, Suzuki H, Toyota M, Watanabe Y, Maruyama R, Sasaki S, et al. Frequent epigenetic inactivation of SFRP genes and constitutive activation of Wnt signaling in gastric cancer. Oncogene 2007.
[70] Marsit CJ, McClean MD, Furniss CS, Kelsey KT. Epigenetic inactivation of the SFRP genes is associated with drinking, smoking and HPV in head and neck squamous cell carcinoma. Int J Cancer 2006;119(8):1761–6.
[71] Cheah PY, Meng YB, Yang X, Kimbrell D, Ashburner M, Chia W. The *Drosophila* l(2)35Ba/nocA gene encodes a putative Zn finger protein involved in the development of the embryonic brain and the adult ocellar structures. Mol Cell Biol 1994;14(2):1487–99.
[72] Nomura M, Zou Z, Joh T, Takihara Y, Matsuda Y, Shimada K. Genomic structures and characterization of Rae1 family members encoding GPI-anchored cell surface proteins and expressed predominantly in embryonic mouse brain. J Biochem (Tokyo) 1996;120(5):987–95.
[73] Cerwenka A, Bakker AB, McClanahan T, Wagner J, Wu J, Phillips JH, et al. Retinoic acid early inducible genes define a ligand family for the activating NKG2D receptor in mice. Immunity 2000;12(6):721–7.
[74] Oppenheim DE, Roberts SJ, Clarke SL, Filler R, Lewis JM, Tigelaar RE, et al. Sustained localized expression of ligand for the activating NKG2D receptor impairs natural cytotoxicity in vivo and reduces tumor immunosurveillance. Nat Immunol 2005;6(9): 928–37.
[75] Gudas LJ, Sporn MB, Roberts AB. Cellular biology and biochemistry of the retinoids. In: Sporn MB, Roberts AB, Goodman DS, editors. The retinoids: biology, chemistry, and medicine. New York: Raven Press; 1994. p. 443–520.
[76] Parrella E, Gianni M, Fratelli M, Barzago MM, Raska Jr I, Diomede L, et al. Antitumor activity of the retinoid-related molecules (E)-3-(4′-hydroxy-3′-adamantylbiphenyl-4-yl)acrylic acid (ST1926) and 6-[3-(1-adamantyl)-4-hydroxyphenyl]-2-naphthalene carboxylic acid (CD437) in F9 teratocarcinoma: role of retinoic acid receptor gamma and retinoid-independent pathways. Mol Pharmacol 2006;70(3):909–24.
[77] Dilworth FJ, Chambon P. Nuclear receptors coordinate the activities of chromatin remodeling complexes and coactivators to facilitate initiation of transcription. Oncogene 2001;20(24):3047–54.

[78] Bastien J, Rochette-Egly C. Nuclear retinoid receptors and the transcription of retinoid-target genes. Gene 2004;328:1–16.
[79] Hauksdóttir H, Privalsky ML. DNA recognition by the aberrant retinoic acid receptors implicated in human acute promyelocytic leukemia. Cell Growth Differ 2001;12:85–98.
[80] Farboud B, Hauksdottir H, Wu Y, Privalsky ML. Isotype-restricted corepressor recruitment: a constitutively closed helix 12 conformation in retinoic acid receptors beta and gamma interferes with corepressor recruitment and prevents transcriptional repression. Mol Cell Biol 2003;23(8):2844–58.
[81] Bruck N, Bastien J, Bour G, Tarrade A, Plassat JL, Bauer A, et al. Phosphorylation of the retinoid x receptor at the omega loop, modulates the expression of retinoic-acid-target genes with a promoter context specificity. Cell Signal 2005;17(10):1229–39.
[82] Eifert C, Sangster-Guity N, Yu LM, Chittur SV, Perez AV, Tine JA, et al. Global gene expression profiles associated with retinoic acid-induced differentiation of embryonal carcinoma cells. Mol Reprod Dev 2006;73(7):796–824.
[83] Niwa H, Miyazaki J, Smith AG. Quantitative expression of Oct-3/4 defines differentiation, dedifferentiation or self-renewal of ES cells. Nat Genet 2000;24(4):372–6.
[84] LaRosa GJ, Gudas LJ. An early effect of retinoic acid: cloning of an mRNA (Era-1) exhibiting rapid and protein synthesis-independent induction during teratocarcinoma stem cell differentiation. Proc Natl Acad Sci USA 1988;85(2):329–33.
[85] Langston AW, Thompson JR, Gudas LJ. Retinoic acid-responsive elements located 3′ of the Hox A and Hox B homeobox gene clusters: functional analysis. J Biol Chem 1997;272:2167–75.
[86] Langston AW, Gudas LJ. Identification of a retinoic acid responsive enhancer 3′ of the murine homeobox gene Hox 1.6. Mech Dev 1992;38:217–28.
[87] Gillespie RF, Gudas LJ. Retinoic acid receptor isotype specificity in F9 teratocarcinoma stem cells results from the differential recruitment of coregulators to retinoic response elements. J Biol Chem 2007;282:33421–34.
[88] Gillespie RF, Gudas LJ. Retinoid regulated association of transcriptional co-regulators and the polycomb group protein SUZ12 with the retinoic acid response elements of Hoxa1, RARbeta(2), and Cyp26A1 in F9 embryonal carcinoma cells. J Mol Biol 2007;372:298–316.
[89] Bastien J, Adam-Stitah S, Riedl T, Egly JM, Chambon P, Rochette-Egly C. TFIIH interacts with the retinoic acid receptor gamma and phosphorylates its AF-1-activating domain through cdk7. J Biol Chem 2000;275(29):21896–904.
[90] Cerignoli F, Guo X, Cardinali B, Rinaldi C, Casaletto J, Frati L, et al. retSDR1, a short-chain retinol dehydrogenase/reductase, is retinoic acid-inducible and frequently deleted in human neuroblastoma cell lines. Cancer Res 2002;62:1196–204.
[91] Kopf E, Plassat JL, Vivat V, de The H, Chambon P, Rochette-Egly C. Dimerization with retinoid X receptors and phosphorylation modulate the retinoic acid-induced degradation of retinoic acid receptors alpha and gamma through the ubiquitin-proteasome pathway. J Biol Chem 2000;275(43):33280–8.
[92] Balmer JE, Blomhoff R. Gene expression regulation by retinoic acid. J Lipid Res 2002;43:1773–808.